INFECTION AND IMMUNITY, May 2005, p. 2628–2643 Vol. 73, No. 5
0019-9567/05/$08.00+0 doi:10.1128/IAI.73.5.2628–2643.2005
Copyright © 2005, American Society for Microbiology. All Rights Reserved.

Microarray and Proteomics Analyses of Human Intestinal Epithelial Cells Treated with the *Aeromonas hydrophila* Cytotoxic Enterotoxin

C. L. Galindo, A. A. Fadl, Jian Sha, L. Pillai, C. Gutierrez, Jr., and A. K. Chopra*

Department of Microbiology and Immunology, The University of Texas Medical Branch, Galveston, Texas 77555-1070

Received 13 October 2004/Returned for modification 6 December 2004/Accepted 21 December 2004

We performed microarray analyses on RNA from human intestinal epithelial (HT-29) cells treated with the cytotoxic enterotoxin (Act) of *Aeromonas hydrophila* to examine global cellular transcriptional responses. Based on three independent experiments, Act upregulated the expression of 34 genes involved in cell growth, adhesion, signaling, immune responses (including interleukin-8 [IL-8] production), and apoptosis. We verified the upregulation of 14 genes by real-time reverse transcriptase-PCR and confirmed Act-induced production of IL-8 by enzyme-linked immunosorbent assay on supernatants from nonpolarized and polarized HT-29 cells. Maximal production of IL-8 in response to Act required the presence of intracellular calcium, since chelation of calcium with BAPTA-AM significantly reduced Act-induced IL-8 production in HT-29 cells. We also examined activation of mitogen-activated protein kinases and, as demonstrated by Western blot analysis of apical side-treated polarized HT-29 cells, Act induced phosphorylation of p38, c-Jun NH_2-terminal kinase, and extracellular signal-regulated kinase 1/2. In addition, KinetWorks proteomics screening of whole-cell lysates revealed Act-induced phosphorylation of cyclic AMP-response element binding protein (CREB), c-Jun, adducin, protein kinase C, and signal transducer and activator of transcription 3 (STAT3) and decreased phosphorylation of protein kinase Bα, v-raf-1 murine leukemia viral oncogene homolog 1 (i.e., Raf1), and STAT1. We verified activation of CREB and activator protein 1 in polarized cells by gel shift assay. This is the first description of human intestinal epithelial cell transcriptional alterations, phosphorylation or activation of signaling molecules, cytokine production, and calcium mobilization in response to this toxin.

Aeromonas hydrophila is a significant human pathogen that causes both gastrointestinal and nonintestinal diseases in children and adults (4, 28). These bacteria are isolated from freshwater, salt water, and a variety of foods (4) and produce an impressive array of virulence factors, including hemolysins, cytotonic and cytotoxic enterotoxins, proteases, lipases, leucocidins, endotoxin, adhesions, and an S-layer (4, 41, 42). Our laboratory isolated and molecularly characterized a cytotoxic enterotoxin (Act) from *A. hydrophila* and subsequently demonstrated that it possessed several biological activities (10). Act causes lysis of red blood cells, is cytotoxic to intestinal and nonintestinal cells, evokes intestinal fluid secretion, and is lethal in nanogram quantities (27 ng) when injected intravenously into mice (4, 10, 60).

The majority of our previous studies focused on macrophage responses to Act, because this toxin caused monocyte/macrophage infiltration into the intestines of animals. Activation of these phagocytic cells contributes to fluid secretory responses and massive inflammation and tissue damage, which are normally associated with *A. hydrophila* infections (60). By using microarrays, we identified cell signaling pathways induced by Act that led to inflammatory responses (7–9) and caused apoptosis of murine RAW 264.7 and peritoneal macrophages (11). Act-induced apoptosis of murine macrophages involved activation of caspases 3, 8, and 9, which was dependent upon the presence of the receptor for tumor necrosis factor alpha (12). Act also caused release of cytochrome *c* and apoptosis-inducing factor from mitochondria, which was not preceded by depolarization of the mitochondrial membrane (12).

Although we clearly demonstrated that Act exerts multiple biological effects on macrophages, intestinal epithelial cell responses to Act are likely important during *Aeromonas*-associated gastroenteritis. Indeed, our previous studies indicated that Act activated mitogen-activated protein kinases (MAPKs) in a human intestinal epithelial cell line (T84) and also caused classical apoptosis of T84 cells, as demonstrated by confocal microscopy and caspase-3 cleavage (12). We further showed Act-induced apoptosis in another human intestinal epithelial cell line (HT-29) by annexin V and propidium iodide staining (12). In order to characterize global transcriptional responses to Act in human intestinal epithelial cells and to better understand host cell signaling, we performed microarray analyses of Act-treated nonpolarized and polarized HT-29 cells. We also used an unbiased proteomics-based approach to identify potential signaling molecules that were phosphorylated or dephosphorylated in response to toxin treatment. In addition, we demonstrated Act-induced production of interleukin-8 (IL-8), which was calcium dependent, and activation of the transcription factors cyclic AMP-response element binding protein (CREB), and activator protein 1 (AP-1) in Act-stimulated HT-29 cells that could play a pivotal role in inducing inflammation and fluid secretory responses.

MATERIALS AND METHODS

Cell culture. The human intestinal epithelial cell line HT-29 was purchased from the American Type Culture Collection (Manassas, VA). These cells have been extensively used as a model system for studying interaction of enteric pathogens or their toxins with intestinal epithelial cells (9, 59, 70). The cells were cultured at 37°C and 5% CO_2 in Dulbecco minimal essential medium (Gibco-

* Corresponding author. Mailing address: Department of Microbiology and Immunology, Medical Research Building, 301 University Blvd., University of Texas Medical Branch, Galveston, TX 77555-1070. Phone: (409) 747-0578. Fax: (409) 747-6869. E-mail: achopra@utmb.edu.

BRL, Gaithersburg, MD) containing 4.5 g of glucose/liter, 10% fetal bovine serum, 2 mM L-glutamine, and the antibiotics penicillin (100 U/ml) and streptomycin (0.1 mg/ml). HT-29 cells are human enterocytes that are relatively undifferentiated when grown under these conditions. For each experiment, 5×10^5 cells/ml were plated in 35-mm dishes and allowed to attach overnight. For apical and basal cell treatments with Act, 5×10^5 cells/ml were polarized by growing for at least 1 week on Costar transwell polycarbonate membrane six-well plate inserts, with a pore size of 0.4 μm (Corning Life Sciences, Acton, MA). The polarized HT-29 cells contain two phenotypes resembling terminally differentiated absorptive enterocytes with properties of Cl^- secretion and mucus-secreting goblet cells. The medium was removed, and fresh medium containing the stimulant (12 ng [unless otherwise stated] of lipopolysaccharide [LPS]-free Act/ml) was added (5) in the upper chamber (apical) or lower chamber (basal) for the indicated times. For calcium chelation experiments, cells were pretreated with the calcium chelator, 1,2-bis(*o*-aminophenoxy)ethane-*N*,*N*,*N*′,*N*′-tetraacetic acid tetra(acetoxy-methyl) ester (BAPTA-AM; 10 μM) for 2 h prior to the addition of Act and remained in the medium throughout the time course of the experiment (54).

Microarray analysis. RNA at 0, 2, and 12 h from Act-treated HT-29 cells was isolated by using the RNAqueous kit (Ambion Austin, TX), and 20 μg of total RNA was processed for microarray analysis. Briefly, cDNA synthesis, in vitro transcription, and labeling and fragmentation to produce the oligonucleotide probes were performed as instructed by the GeneChip manufacturer (Affymetrix, Santa Clara, CA). The probes were first hybridized to a test array (Affymetrix) and then to the GeneChip human genome HU133A; both were performed using the GeneChip Hybridization Oven 640. The chips were washed in a GeneChip Fluidics Station 400 (Affymetrix), and the results were visualized with a Gene Array scanner using Affymetrix software. The data were analyzed by using GeneChip Operating Software (GCOS; Affymetrix), Significance Analysis of Microarrays (SAM; Stanford University, Stanford, CA) (30), Spotfire DecisionSite 7.3 (Spotfire, Inc., Somerville, MA), and analysis of variance (ANOVA; Spotfire DecisionSite 7.3). Computational hierarchical cluster analysis was performed by using Spotfire DecisionSite 7.3, Cluster/Treeview (Eisen Laboratory, University of California, Berkeley, CA) (40), CLUSFAVOR 6.0 (Baylor College of Medicine, Houston, TX), and ArrayMiner5 (Optimal Design, Belgium).

Real-time RT-PCR. Real-time quantitative reverse transcriptase PCR (RT-PCR) was performed in the LightCycler thermal cycler system (Roche Diagnostics, Indianapolis, IN) with SYBR Green I dye (Qiagen, Valencia, CA) as described by the manufacturer. Briefly, 200 ng of RNA was placed into a 20-μl reaction volume containing 1 μg of each primer, 10 μl of SYBER Green PCR master mix, and 0.2 μl of reverse transcriptase. A typical protocol included reverse transcription at 55°C for 20 min and a denaturation step at 95°C for 15 min, followed by 40 cycles with 95°C denaturation for 15 s, 55°C annealing for 20 s, and 72°C extension for 20 s. The temperature transition rate was set at 20°C per s. Detection of the fluorescent product was performed at the end of the extension period at 80°C for 10 s. To confirm amplification specificity, the PCR products were subjected to a melting curve analysis. Negative controls containing water instead of RNA were concomitantly run to confirm that the samples were not cross-contaminated. Targets were normalized to reactions performed by using glyceraldehyde-3-phosphate dehydrogenase (GAPDH) amplimers (Biosource, Camarillo, CA), and the fold change was determined with the LightCycler analysis software, as previously described (72).

Cytokine profiles. Bio-Plex cytokine assays (Bio-Rad, Richmond, CA) were performed by the Gastrointestinal Immunology Core of the Texas Gulf Coast Digestive Diseases Center (University of Texas Medical Branch at Galveston) as described by the manufacturer. Briefly, 50 μl of cytokine standards or samples (supernatant from Act-treated cells) were incubated with 50 μl of anti-cytokine conjugated beads in 96-well filter plates for 30 min at room temperature with shaking. Plates were then washed by vacuum filtration three times with 100 μl of Bio-Plex wash buffer, 25 μl of diluted detection antibody was added, and plates were incubated for 30 min at room temperature with shaking. After three filter washes, 50 μl of streptavidin-phycoerythrin was added, and the plates were incubated for 10 min at room temperature with shaking. Finally, plates were washed by vacuum filtration three times, beads were suspended in Bio-Plex assay buffer, and samples were analyzed on a Bio-Rad 96-well plate reader.

ELISA. Levels of IL-8 in tissue culture supernatants from Act-treated HT-29 cells were determined by enzyme-linked immunosorbent assay (ELISA) according to our published procedure (61). Briefly, high-binding microtiter plates were coated with purified anti-cytokine capture antibodies and incubated overnight at 4°C. After washing and blocking, samples or standards were added, followed by washing with phosphate-buffered saline (PBS)–Tween (0.1%). Detection antibodies were added and incubated for 45 min at room temperature. Plates were then washed, and an enzyme conjugate (streptavidin-conjugated horseradish peroxidase) was added and incubated at room temperature for 30 min. After washing, ABTS [2,2′azinobis(3-ethylbenzthiazolinesulfonic acid)] substrate was added, and the optical density was read with an ELISA plate reader (Molecular Devices Corp., Sunnyvale, CA) at 405 nm.

Western blot analysis. Antibodies were purchased from Cell Signaling Technology (Beverly, MA), and Western blot analysis was performed by established procedures (56) with slight modifications according to specifications of the antibody manufacturer. Briefly, equal amounts of total protein were loaded and separated on sodium dodecyl sulfate (SDS)–10% polyacrylamide gels and then transferred to nitrocellulose membranes. Membranes were blocked with 5% milk and washed in 1× Tween (0.1%)–Tris-buffered saline (TTBS) three times for 5 min each time. Primary antibodies diluted 1:1,000 in 5% milk or bovine serum albumin (prepared in 1× TTBS) were allowed to incubate overnight at 4°C. After washing, horseradish peroxidase-conjugated secondary antibody (Cell Signaling Technology) was diluted 1:2,000 in 5% milk and applied to the membranes. Subsequently, membranes were washed and a chemiluminescence substrate (Pierce Biotechnology, Rockford, IL) was applied and allowed to incubate at room temperature for 5 min, before the membranes were exposed to X-ray films (12).

Phosphoprotein screens. Whole lysate protein samples (500 μg) from Act-treated (12 or 50 ng/ml) HT-29 cells (nonpolarized or polarized) were analyzed by using KinetWorks KPSS-1.3 phosphorylation screens (Kinexus Bioinformatics Corp., Vancouver, British Columbia, Canada) as described by the manufacturer. The KinetWorks analysis, which was performed by Kinexus, involved resolution of a single lysate sample by SDS-polyacrylamide gel electrophoresis (PAGE) and subsequent immunoblotting with panels of up to three primary antibodies per channel in a 20-lane Immunetics Multiblotter. The antibody mixtures were carefully selected to avoid overlapping cross-reactivity with target proteins. Normalized trace quantity units (cpm) were arbitrary based on the intensity of fluorescence detection for target immunoreactive proteins recorded with a Fluor-S MultiImager and quantified by using Quantity One Software (Bio-Rad) (12). Kinexus performed all of the normalization and statistical analysis on the data.

Gel shift analysis. Gel shift assays were performed as previously described (13). Briefly, consensus oligonucleotide for CREB or AP-1 was labeled by using T4 polynucleotide kinase (Promega, Madison, WI) according to the instructions of the manufacturer. Next, DNA-binding reaction mixtures were assembled. We used unlabeled CREB or AP-1 consensus oligonucleotide as a specific competitor, unlabeled NF-κB consensus oligonucleotide as a nonspecific competitor (Promega), and nuclear extracts from specific time points after Act treatment (50 ng/ml) of polarized HT-29 cells (apical side). Nuclear extracts were prepared by using NE-PER kit (Pierce Biotechnology) as described by the manufacturer. The reaction mixtures were incubated at room temperature for 10 min, followed by the addition of 20,000 cpm of ^{32}P-labeled transcription factor consensus oligonucleotide and incubation for 20 min at room temperature. Subsequently, 1 μl of gel loading 10× buffer (Promega) was added to each reaction mixture, and samples (5 μg) were loaded on a nondenaturing 4% polyacrylamide gel. The gel was prerun in 0.5× Tris-borate-EDTA buffer for 30 min at 35 mA before the samples were loaded. After completion of the run, the gel was transferred to Whatman 3MM paper, dried at 80°C for 5 h, and exposed to X-ray film overnight to 48 h.

Calcium mobilization. Calcium mobilization experiments were performed essentially as previously described (54). Briefly, HT-29 cells (10^6 cells/ml) in calcium-free Dulbecco modified Eagle medium containing 10% fetal bovine serum were loaded with 5 nM Fura 2-AM and 0.8 mM pluronic. Cells were protected from light, vortexed briefly, and then incubated at 37°C for 1 h. Subsequently, cells were centrifuged at 3,000 rpm for 5 min and then washed three times with Hank's buffered salt solution (Sigma, St. Louis, MO). An aliquot of the cell suspension (1.5 ml) was read in a Hitachi (Naperville, IL) F-2500 fluorescence spectrophotometer for 300 s. Act (2.3 μg/ml) was added after a basal fluorescence level for the cells was achieved. At the end of the experiment, 1 μM ionomycin and 67 μM EGTA were added to measure, respectively, the maximum and minimum calcium release from cells.

All of the experiments were performed at least in triplicate, and representative data are presented. Where applicable, the data were plotted as arithmetic mean ± the standard deviation, and the Student *t* test ($P \leq 0.05$) was used for data analysis.

RESULTS

Act induces upregulation of gene transcription in human intestinal epithelial cells. HT-29 cells were treated with a sublethal dose of Act (12 ng/ml) for 0, 2, and 12 h (in triplicate),

and the RNA was isolated and applied to HU133 GeneChips, as previously described (13). In addition, one experiment (0 and 2 h) of Act-treated (12 ng/ml) polarized HT-29 cells was performed. Because the host cell receptor for Act could be distributed on either the apical or basolateral surface, polarized cells were treated with the toxin on both sides (apical and basal). The data were analyzed separately using four different techniques: GCOS, SAM, Spotfire 7.3, and ANOVA (13). We expected a fold change of at least 2.0 as significant for Act-treated nonpolarized HT-29 cells (13). However, we expected a fold change value of $\geq$1.5 to be significant for polarized cells, partly because gene expression changes in these cells were only deemed significant if they also occurred in nonpolarized cells. We also lowered the fold change expectation for polarized cells due to the fact that alterations in gene expression were generally lower in these cells compared to those of nonpolarized cells. However, we later noted that polarized cells responded more similarly to nonpolarized cells when higher doses of Act were used, possibly due to the physical nature of polarized cell monolayers with tight junctions.

Genes that were deemed significant by all four analysis techniques were compiled into a list that included 45 probe sets representing 34 genes for 0- versus 2-h treatments of nonpolarized cells (Table 1). Affymetrix GeneChip probe sets are 25 nucleotides long, and many genes are represented by two or more different probe sets that depict different portions of the same gene sequence (Affymetrix). We considered our data to be highly consistent, because Act upregulated three separate probe sets representing Jagged 1 and four different probe sets representing myeloid cell leukemia cell sequence 1 (Mcl-1) or T-cell death-associated gene 51 (TDAG51). Surprisingly, there were no downregulated genes that were deemed significant based on our analysis methods.

Based on microarray analysis results (Table 1), Act significantly upregulated genes in epithelial cells that coded for proteins involved in cell cycle regulation (e.g., cyclin-dependent kinase inhibitor 1A [p21/Cip1], dickkopf homolog 1, and jagged 1) and apoptosis (e.g., Mcl-1 and TDAG51). There were three genes, encoding matrix metalloproteinase 1 (MMP1), soluble urokinase plasminogen activator receptor, and urokinase-type plasminogen activator receptor, involved in extracellular matrix digestion, that were upregulated by Act. Act also induced upregulation of three genes encoding proteins involved in cellular reorganization (e.g., actin), migration, and cell-cell communication: gap junction protein, beta 3 (connexin 31), cytokeratin, and ras homolog gene family, member E (RhoE) (Table 1). There were several signaling molecules and transcription factors that were upregulated in HT-29 cells in response to Act by 2 h, including the AP-1 transcription factor subunit Fra-1. Likewise, four cytokines (cardiotrophin-like cytokine, GRO1, IL-8, and leukemia inhibitory factor [LIF]) were up regulated by Act in these epithelial cells, based on microarray analysis results (Table 1). The expression of only one gene (MMP1) was significantly altered by Act between 0 and 12 h, based on all four analyses techniques used (GCOS, SAM, Spotfire, and ANOVA). MMP1 was upregulated by averages of 4.2-fold at 2 h (Table 1) and 6.2-fold at 12 h (data not shown).

Genes from polarized cells exhibited a similar pattern of expression alteration in response to Act treatment (Table 1). Only 5 of the 34 upregulated genes from Act-treated nonpolarized intestinal epithelial cells were not significantly altered in toxin-treated polarized cells (i.e., dickkopf homolog 1, growth differentiation factor 15, growth-related oncogene 1 [GRO1], ADP-ribosylation factor 2, and cytokeratin 17). The reason for these differences is unclear but could represent differential expression of genes in polarized versus nonpolarized cells, which requires further investigation.

Confirmation of Act-induced upregulation of genes in human intestinal epithelial cells by real-time RT-PCR. In order to confirm the microarray data, real-time RT-PCR was performed on selected genes (Table 2). Experiments were run in parallel, and the fold change values were determined after normalization of each gene to GAPDH by using the comparative threshold method (37). We chose 14 genes for verification (Tables 1 and 2) based on their known involvement in stress and/or apoptosis, cell cycle regulation, extracellular matrix digestion, and intracellular signaling related to immune responses. As shown in Table 1, Mcl-1 and TDAG51 were upregulated in nonpolarized HT-29 cells 2.3- to 2.5-fold and 5.5- to 6.4-fold, respectively, according to microarray analyses, and we verified the upregulation of Mcl-1 (2.4-fold) and TDAG51 (16.7-fold) by real-time RT-PCR (Table 2). Likewise, real-time RT-PCR verified Act-induced upregulation of the other 12 genes. (Table 2). Verification of Act-induced upregulation of genes in polarized cells yielded similar results. As expected, induction of GRO1 was not observed in toxin-treated polarized HT-29 cells, as also demonstrated by the microarray analyses (Tables 1 and 2). It is worth mentioning that the fold changes for IL-8 in Act treated HT-29 cells by microarray analysis were determined to be 21.8 to 31.6 and only 2.4 by real-time RT-PCR. Likewise, for LIF the fold change was 2.5 to 2.8 by microarray analysis and 14.6 by real-time RT-PCR (Table 2). One of the possible reasons for the discrepancies in the actual numbers is the nature of the two different techniques. For instance, the microarrays utilize probe sets (25 bp), whereas the real-time RT-PCR technique depends upon the nature of the primers and their locations and lengths.

We used the gene-encoding GAPDH as an internal control because its level remained unchanged for up to 2 h of treatment with Act in HT-29 cells. A slight (1.2- to 1.3-fold) but statistically insignificant increase in the levels of GAPDH mRNA was noted at 12 h based on microarray analysis. However, it could not be confirmed by real-time RT-PCR. Similar small and statistically insignificant increases in GAPDH transcript were also noted at 12 h in RAW 264.7 murine macrophages (13).

Act-induced genes follow a similar pattern of expression in human intestinal epithelial cells. To identify groups of genes with similar expression patterns, we used four separate software programs to perform hierarchical clustering: Cluster/Treeview, CLUSFAVOR 6.0, Spotfire DecisionSite 7.3, and ArrayMiner5. Example clusters are shown in Fig. 1A (CLUSFAVOR) and B (Spotfire). Notably, all three 0-h time points clustered together, and all three 2-h time points clustered together (Fig. 1B), indicating consistency between the three experiments, for this particular group of 200 genes (Fig. 1B). Furthermore, the average expression levels of the genes in this cluster were very similar for the independent experiments, as

TABLE 1. Most significant genes upregulated by Act in human intestinal epithelial cells (HT-29) from 0 to 2 h as determined by four separate analysis methods (grouped by function)[a]

GenBank no.	Gene name	Nonpolarized				Polarized, GCOS (FC)
		GCOS (FC)	SAM (FC)	Spotfire (FC)	ANOVA (*P*)	
Apoptosis						
BF594446	Myeloid cell leukemia sequence 1 (Bcl-2-related)	2.6	2.7	2.6	0.013611	5.3
NM_021960.1	Myeloid cell leukemia sequence 1 (Bcl-2-related)	2.5	2.5	2.3	0.018607	4
BF981280	Myeloid cell leukemia sequence 1 (Bcl-2-related)	2.4	3.2	3.0	0.001319	1.9
AI275690	Myeloid cell leukemia sequence 1 (Bcl-2-related)	2.1	2.4	2.3	0.014808	2.8
NM_007350.1	TDAG51	5.5	6.2	6.4	0.01555	3
AI795908	TDAG51	4.7	4.8	4.6	0.00381	4
AA576961	TDAG51	4.3	4.3	4.1	0.008432	4
NM_007350.1	TDAG51	2	2.2	2.2	0.007025	1.6
Cellular reorganization						
AF099730	Gap junction protein, beta 3 (connexin 31)	2.3	2.1	2.1	7.66E-06	2.1
BF060667	Gap junction protein, beta 3 (connexin 31)	2.2	2.1	2.2	1.15E-06	2.3
Z19574	Cytokeratin 17	2.2	2.4	2.5	5.31E-20	NS
BG054844	Ras homolog gene family, member E (RhoE)	2.2	2.1	2.1	0.001669	1.6
Cell growth/Differentiation/Cell cycle regulation						
NM_000389.1	Cyclin-dependent kinase inhibitor 1A (p21, Cip1)	3.1	2.3	2.3	0.002638	3.2
NM_012242.1	Dickkopf homolog 1 (DKK1)	2.8	2.7	2.6	0.000874	NS
NM_001432.1	Epiregulin	2.7	2.9	2.8	0.012219	2.1
AF003934.1	Growth differentiation factor 15 (GDF15)	2.3	2.2	2.5	0.008893	NS
U77914.1	Jagged 1 (JAG1)	2.2	2.5	2.5	0.000286	1.7
U61276.1	Jagged 1 (JAG1)	2.1	2	2.1	6.33E-05	1.9
U73936.1	Jagged 1 (JAG1)	2.1	2.5	2.5	0.000304	1.7
NM_002467.1	Myc proto-oncogene protein (c-Myc)	2.1	2.3	2.2	0.013804	1.5
AF045451.1	NGFI-A binding protein 1 (Nab1)	3	3.3	3.3	0.015786	1.7
NM_002607.1	Platelet-derived growth factor alpha polypeptide	2.4	2.3	2.2	0.006248	1.5
AI263909	Ras homolog gene family, member B (RhoB)	2.7	2.9	2.8	0.001791	3.2
NM_023925.1	C1q domain containing 1	2.1	2	2.0	0.004791	2
Cytokines						
NM_013246.1	Cardiotrophin-like cytokine; neurotrophin-1B-cell stimulating factor-3 (CLC)	2.5	2.3	2.6	0.00929	2.6
NM_001511.1	GRO1 oncogene	3.1	4.2	4.4	0.00368	NS
AF043337.1	IL-8	31.6	24.3	32.9	0.006866	1.9
NM_000584.1	IL-8	26.4	23.8	21.8	0.010181	3
NM_002309.2	Leukemia inhibitory factor (LIF)	2.5	2.7	2.8	0.007476	2.3
Extracellular matrix digestion						
NM_002421.2	Matrix metalloproteinase 1 (MMP1)[b]	4	4.5	4.0	0.035324	2.6
AY029180.1	Soluble urokinase plasminogen activator receptor	2.1	2.4	2.3	0.006765	1.9
U08839.1	Urokinase-type plasminogen activator receptor	2	2	2.0	0.022107	1.7
Signal transduction						
U16996.1	Dual specificity protein phosphatase 5	2.1	2	2.0	0.00587	4
NM_004431.1	Ephrin type-A receptor 2 (EphA2)	2.7	3.1	3.0	0.006323	2.6
U16797.1	Ephrin-B2	2.6	2.2	2.3	0.005556	2.8
BF001670	Ephrin-B2	2.1	2.1	2.2	0.006585	2.5
NM_002923.1	Regulator of G-protein signaling 2 (RGS2)	4.2	3.8	3.6	0.005268	2.8
Transcription factors						
AL564683	CCAAT enhancer binding protein (CEBP), beta	2	2.1	2.0	0.029667	3.2
BG251266	Fra-1	5.2	5.3	5.9	0.001552	12.1
AL021977	MAFF-like protein	3.2	2.7	3.3	0.003684	1.7
NM_014755.1	SERTA domain containing 2	2	2	2.0	0.018674	2
Other/unknown						
NM_025047.1	ADP-ribosylation factor 2 (cDNA, 79%)	2.3	2.6	2.5	0.000746	NS[c]
NM_000693.1	Aldehyde dehydrogenase 1 family, member A3	2.4	2.6	2.4	0.04679	2.1
NM_006033.1	Endothelial lipase	2.7	3.2	2.9	0.023085	1.6
NM_001450.1	LIM-protein 3	2.2	2.3	2.2	0.009135	1.6

[a] FC, fold change. Genes listed twice were represented on the microarrays by more than one probe set, and each was determined separately to be significantly upregulated by Act.

[b] Also upregulated between 0 and 12 h, as determined by all four analysis techniques.

[c] NS, no significant change.

TABLE 2. Confirmation by real-time RT-PCR of selected genes determined to be upregulated by Act in human intestinal epithelial cells (HT-29) by using microarrays

GenBank no.	Gene name	Fold change[a]			
		Nonpolarized		Polarized	
		Microarrays (0 vs 2 h)	RT-PCR (0 vs 2 h)	Microarrays (0 vs 2 h)	RT-PCR (0 vs 2 h)
NM_021960.1	Mcl-1	2.3–2.5	2.4	1.9–5.3	2.8
NM_007350.1	TDAG51	5.5–6.4	16.7	1.6–4.0	7.8
NM_000389.1	Cip1	2.3–3.1	14.3	3.2	6.9
NM_002467.1	c-Myc	2.1–2.3	2.4	1.5	2.1
AF045451.1	Nab1	3.0–3.3	2.7	1.7	2.5
NM_013246.1	Cardiotrophin-like cytokine	2.3–2.6	5.4	2.6	4.2
NM_001511.1	GRO1	3.1–4.4	10.1	NC[a]	NC
NM_000584.1	IL-8	21.8–31.6	2.4	1.9–3.0	2.1
NM_002309.2	LIF	2.5–2.8	14.6	2.3	2.9
NM_002421.2	MMP1	4.0–4.5	6.9	2.6	5.8
NM_004431.1	EphA2	2.7–3.1	11.5	2.6	3.9
U16797.1	Ephrin-B2	2.2–2.6	4.7	2.5–2.8	2.8
NM_002923.1	Rgs2	3.6–4.2	6.2	2.8	4.1
BG251266	Fra-1	5.2–5.9	2.9	12.1	7.5

[a] NC, no change.

shown graphically in Fig. 1A. There were eight probe sets representing seven genes that consistently clustered together that were also considered significant by four analyses techniques: GCOS, SAM, Spotfire DecisionSite, and ANOVA (Fig. 1C). Six of the coclustered genes were involved in cellular reorganization (i.e., connexin 31, cytokeratin 17, RhoE, and jagged 1) or cell growth (i.e., p21/Cip1, dickkopf homolog 1, and jagged 1).

Cytokine profile analysis of Act-treated human intestinal epithelial cells. To determine which cytokines were indeed produced in response to Act, we performed a broad cytokine profile analysis on supernatants of Act-treated nonpolarized HT-29 cells. We chose a later time point than that used for microarray analyses (12 h) in order to examine levels of secreted proteins. There was no significant production of IL-2, IL-4, IL-5, IL-6, IL-7, IL-10, IL-12, IL-13, IL-17, granulocyte-colony stimulating factor, granulocyte-macrophage colony stimulating factor, gamma interferon, tumor necrosis factor alpha, IL-1β, monocyte chemoattractant protein 1, or macrophage inflammatory protein 1β in response to Act (data not shown). However, Act induced production of IL-8 (952 pg/ml) in nonpolarized HT-29 cells (data not shown), which supported the microarray analysis results (Table 1).

Act induces IL-8 production in polarized human intestinal epithelial cells. In vivo, intestinal epithelial cells are polarized, and many membrane receptors are localized to either the apical or basolateral side of each cell. In order to determine from which side of intestinal epithelial cells that Act might initiate host signaling, we performed ELISA of supernatants from either the apical or basal side of toxin-treated (12, 50, or 100 ng of Act/ml for 12 or 24 h) polarized epithelial cells. We used higher doses of Act (50 and 100 ng/ml), since these concentrations could be biologically relevant. Further, we intended to establish a dose-response effect of Act on IL-8 production in HT-29 cells. As shown in Fig. 2A, Act induced production of IL-8, which increased with dose, from apical side-treated HT-29 cells by 12 h. There was some production of IL-8 in basal side-treated cells by 24 h, but it was much lower than that from cells treated on the apical side (Fig. 2B).

Act induces activation of MAPK signaling cascades via phosphorylation of ERK 1/2, p38 kinase, and JNK in human intestinal epithelial cells. Polarized HT-29 cells were treated on the apical side with 50 ng/ml of Act for various time points, and whole-cell lysates were subjected to electrophoresis and Western blot analysis. LPS-treated RAW 264.7 cells (100 ng/ml for 30 min) were used as a positive control because LPS has been shown to induce ERK, p38 kinase, and JNK pathways in RAW 264.7 murine macrophages (57). Subsequent blots were probed with antibodies specific for the phosphorylated form of ERK 1/2 (p-ERK), JNK (p-JNK), or p38 (p-p38). Blots were also probed with total ERK, JNK, or p38 antibodies, which recognized both phosphorylated and nonphosphorylated forms, to control for protein loading. As shown in Fig. 3A, Act induced two bands (44 and 42 kDa), a finding consistent with the phosphorylated forms of ERK 1 and 2 by 2 h. Increased phosphorylation of ERK 1/2 observed upon Act treatment was not due to an increase in the protein concentration of ERK 1/2, as evidenced by similarly sized bands for each time point when blots were probed with total ERK 1/2 antibody (data not shown). Likewise, Act induced phosphorylation of JNK and p38 kinase in apical side-treated intestinal epithelial cells, although induction occurred later (4 h, Fig. 3B and C). An increase in total protein concentration was not observed for either JNK (data not shown) or p38 kinase (Fig. 3D). The data demonstrated for the first time activation of these kinases in polarized epithelial cells. In a previous study, we showed activation of these kinases in macrophages and in nonpolarized T84 epithelial cells (12).

Act induces phosphorylation of multiple intracellular signaling molecules in human intestinal epithelial cells. In order to further characterize intestinal epithelial cell responses to Act, we undertook an unbiased proteomics-based approach to discover which proteins might mediate Act-induced host cell signaling. HT-29 cells (nonpolarized) were treated with PBS or Act (12 ng/ml) for 2 h, and whole-cell lysates (500 μl [1 mg/ml] per treatment) were applied to KinetWorks Phosphoprotein Screens in order to analyze the expression profiles of 31 intracellular signaling proteins. We compared normalized trace

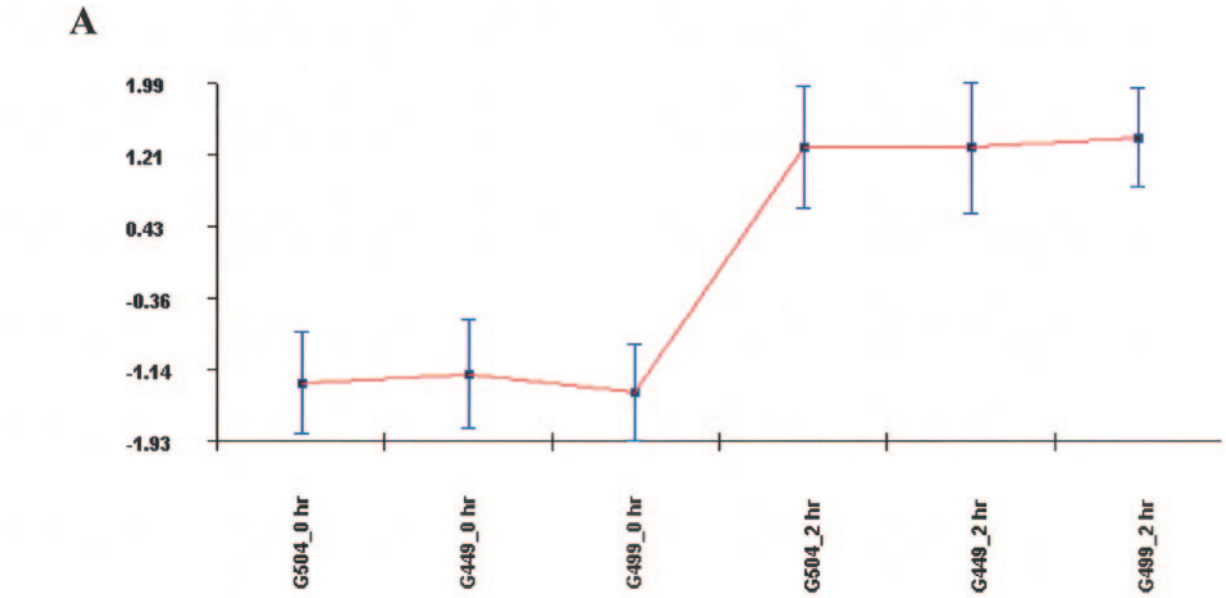

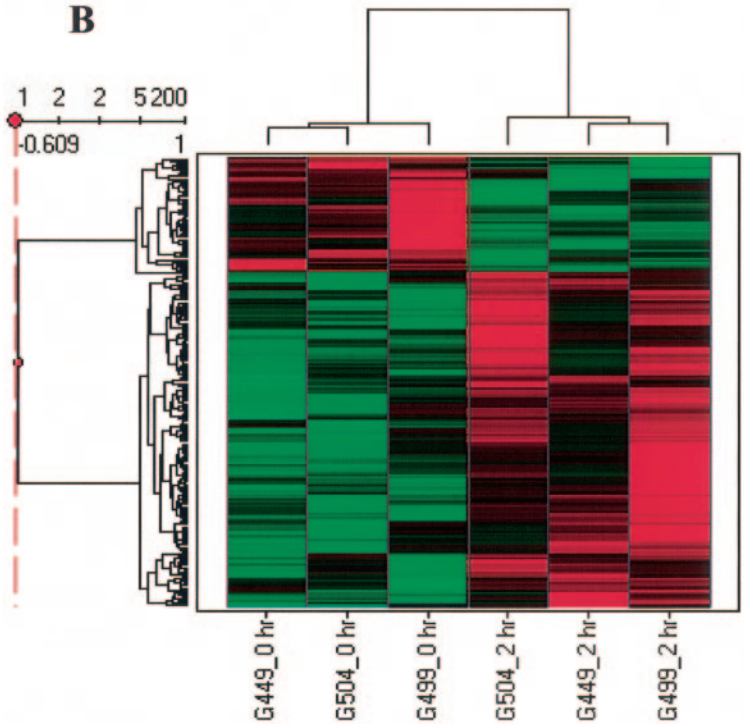

C

GenBank ID	Gene name
AF099730	Connexin 31
BF060667	Connexin 31
Z19574	Cytokeratin 17
BG251266	Fra-1
BG054844	RhoE
NM_000389.1	p21, Cip1
U73936.1	Jagged 1
NM_012242.1	Dickkopf homolog 1 (DKK1)

FIG. 1. Hierarchical clusters of genes from Act-treated intestinal epithelial cells (HT-29). Hierarchical cluster analysis was performed on signal values from six arrays (0 and 2 h replicate experiments) using CLUSFAVOR 6.0, Spotfire DecisionSite 7.3, and Arrayminer5. The Cluster/Treeview software programs were used to cluster fold change values generated from three experimental comparisons with human intestinal epithelial cells (3 replicates of 0 versus 2 h). (A) Graphical representation of a cluster generated by using CLUSFAVOR 6.0 that represents a set of genes upregulated by 2 h in Act-treated human intestinal epithelial cells. Normalized intensity values are displayed on the ordinate, and the abscissa represents each experiment. G449, G499, and G504 represent the three independent experimental array sets (0 and 2 h) with human intestinal epithelial cells. (B) Clustering generated by using Spotfire DecisionSite 7.3 showing a set of upregulated genes (similar to that generated by CLUSFAVOR 6.0). Higher signal values are shown in red, and lower signal values are shown in green. Black represents median signal values. (C) List of genes upregulated by 2 h specifically in Act-treated human intestinal epithelial cells that clustered together for all four clustering programs used (Cluster/Treeview, CLUSFAVOR 6.0, Spotfire DecisionSite 7.3, and ArrayMiner5).

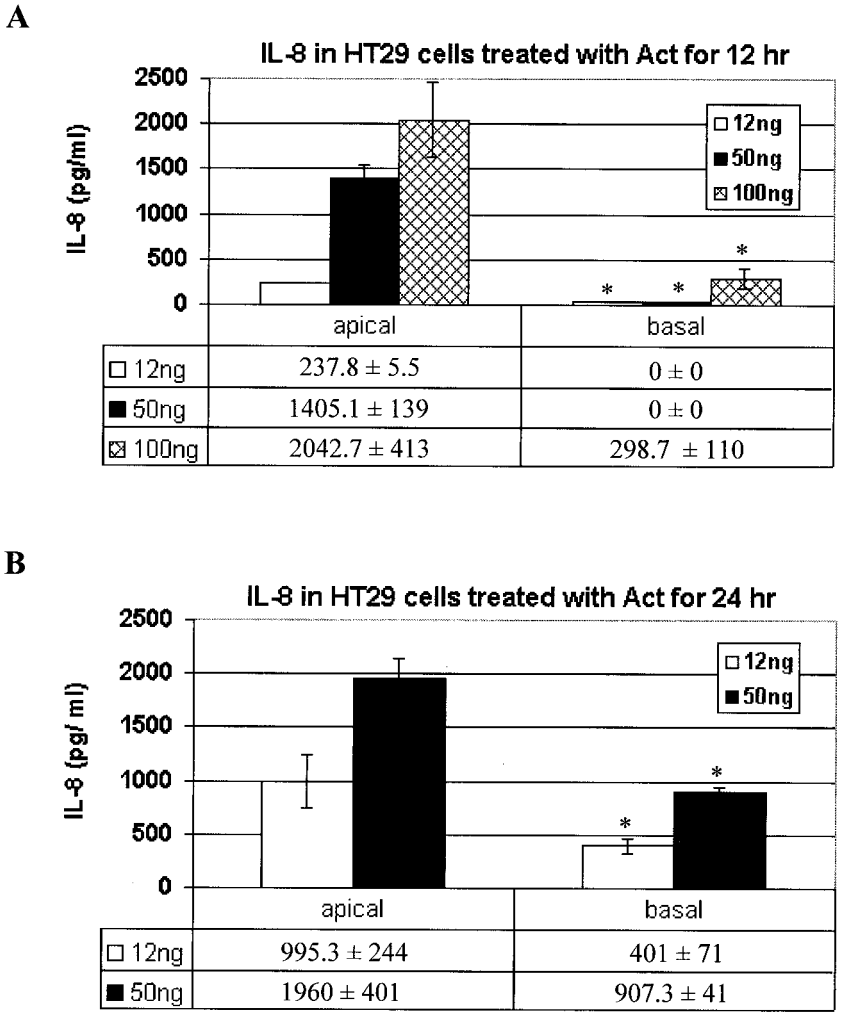

FIG. 2. IL-8 production in Act-treated polarized intestinal epithelial cells (HT-29). ELISAs (Bio-Rad) were performed on the supernatants of Act-treated human intestinal epithelial cells (0, 12, and 24 h). Concentration of IL-8 is shown on the ordinate, treatment application (apical or basal side) is displayed on the abscissa, and a table below each graph displays the actual, normalized concentration (pg/ml) of each cytokine. Error bars are based on standard deviations calculated for three separate experiments. (A) IL-8 production for HT-29 cells apically or basally treated for 12 h. (B) IL-8 production for HT-29 cells apically or basally treated for 24 h. Asterisks denote statistically significant values between apical side- versus basal side-treated polarized cells at various toxin concentrations.

quantity units (cpm), arbitrarily based on the fluorescence intensity values, and considered a 25% increase or decrease in expression to be significant. Of the 31 proteins screened (data not shown), 4 were significantly upregulated (e.g., p38 kinase, adducin, CREB, and retinoblastoma protein [Rb]) and three downregulated (e.g., Raf1, PKBα/Akt, and *N*-methyl-D-aspartate [NMDA] glutamate receptor subunit [NR1]) by Act at 2 h (Fig. 4A and B and 5A and B). Immunoblots including these seven proteins are shown in Fig. 4A (0 h) and B (2 h) for comparison, and the data are graphically represented, along with percentage increases or decreases in Fig. 5A and B.

We also performed phosphoprotein screens on whole-cell lysates (0 and 4 h) from apical side-treated (50 ng/ml of Act) polarized intestinal epithelial cells (Fig. 4C, 4D, 5A, and 5B). We chose a higher dose of Act for polarized cells, because IL-8 production in polarized cells treated on the apical side with 50 ng/ml of Act (1405.1 pg/ml, Fig. 2A) was comparable to nonpolarized cells treated with 12 ng/ml of Act (952 pg/ml, data not shown). We chose the later time point (4 h), because Western blot analyses of lysates from apical side-treated polarized HT-29 cells revealed phosphorylation of JNK and p38 kinase at 4 h (Fig. 3B and C). Considered together, the data (Act-induced IL-8 production and MAPK phosphorylation) suggested that polarized cells were less responsive to low levels of toxin than nonpolarized cells.

Act induced phosphorylation of ERK 1 (443%), ERK 2 (530%), and c-Jun (496%), a phosphorylation target of JNK, by 4 h in polarized intestinal epithelial cells (Fig. 4C and D and 5A). ERK 2 was only minimally phosphorylated (11%) in toxin-treated nonpolarized cells. Phosphorylation of p38 kinase, however, was induced by Act by 2 h in nonpolarized HT-29 cells but not in polarized cells (Fig. 4A to D and 5A). Phosphorylation of Raf-1 was downregulated in both nonpolarized (−31%) and apical-treated polarized (−36%) cells in response

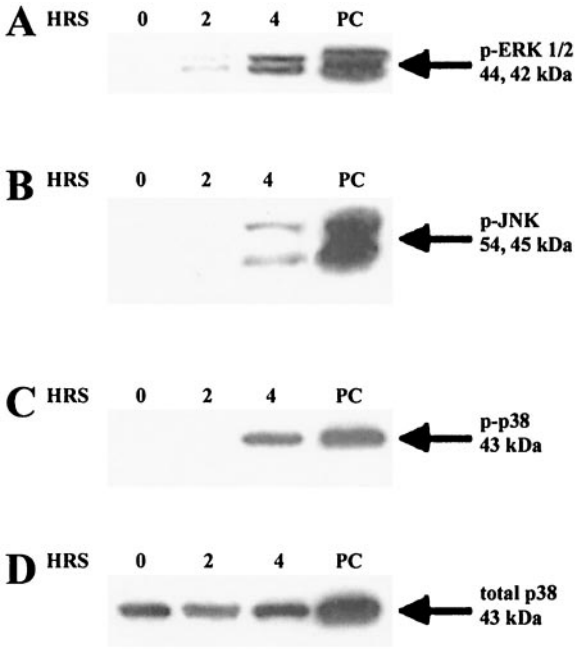

FIG. 3. Act-induced phosphorylation of ERK, JNK, and p38 kinase in Act-treated human intestinal epithelial cells (HT-29). Polarized cells were stimulated on the apical side with Act (50 ng/ml) for the indicated times, cells were lysed, and Western blot analysis was performed with anti-phospho-ERK 1/2 (p-ERK 1/2), p-JNK, or p-p38 antibody. Blots were probed with anti-p38 (total p38) antibody as a control for protein loading. (A) Western blot analysis of apical (Act)-treated polarized intestinal epithelial cells with p-ERK antibody. (B) Western blot analysis of apical side (Act)-treated polarized intestinal epithelial cells with p-JNK antibody. (C) Western blot analysis of apical side (Act)-treated polarized intestinal epithelial cells with p-p38 antibody. (D) Western blot analysis of apical side (Act)-treated polarized intestinal epithelial cells with total p38 antibody.

to Act (Fig. 4A to D and 5A). As shown in Fig. 4A to D and 5B, Act caused upregulation of phosphorylated adducin (28%) by 2 h in nonpolarized HT-29 cells, which also occurred, to a greater extent, in apical-treated polarized cells (134%). Act also upregulated phosphorylation of the transcription factor CREB in nonpolarized (254%) and polarized (106%) intestinal epithelial cells (Fig. 4A to D and 5B).

Act caused downregulation of phosphorylated PKBα (also called Akt1) in toxin-treated nonpolarized HT-29 cells (−47%, Fig. 4A, 4B, and 5B) and also in polarized cells, albeit at a lower level (−7%). As shown in Fig. 4C, 4D, and 5B, Act increased phosphorylation of PKCα (128%) and PKCδ (110%) in apical side-treated polarized intestinal epithelial cells but not in nonpolarized cells (Fig. 5B). Act treatment caused a decrease in signal transducer and activator of transcription 1 (STAT1) phosphorylation (−39%) and an increase in STAT3 phosphorylation (28%) in polarized HT-29 cells (Fig. 4C, 4D, and 5B). However, there were no changes in STAT1 or STAT3 phosphorylation in nonpolarized HT-29 cells.

There were two proteins for which Act treatment produced conflicting results in nonpolarized and apical-treated polarized cells: NR1 and Rb. NR1 was highly upregulated in polarized cells (102%) and downregulated in nonpolarized cells (−56%) in response to Act treatment. Likewise, Act caused upregulation of phosphorylated Rb in nonpolarized cells (137%) and downregulation in apical side-treated polarized cells (−63%) (Fig. 4A to D and 5B).

Act activates the transcription factors CREB and AP-1 in polarized human intestinal epithelial cells. Act-induced phosphorylation of CREB was observed for both nonpolarized and polarized human intestinal epithelial cells (Fig. 4A to D and 5B). In order to verify transcription factor activity of CREB, we performed gel shift assays, with a labeled consensus sequence specific for CREB, on nuclear extracts from polarized HT-29 cells treated with Act on the apical side. Figure 6 clearly demonstrates that Act caused nuclear translocation of a protein capable of binding a radiolabeled CREB binding sequence. The binding was evident between 30 min to an hour and persisted to at least 4 h. We also performed competition assays with unlabeled CREB (specific) or NF-κB (nonspecific) consensus oligonucleotides. As shown in Fig. 6A, addition of the specific competitor ablated binding, whereas the nonspecific competitor did not, indicating that the band observed was indeed specific for CREB.

We previously demonstrated Act-induced AP-1 transcription factor activation in RAW 264.7 murine macrophages, by gel shift assay. In the present study we demonstrated Act-induced transcriptional upregulation of the AP-1 subunit Fra-1 in both nonpolarized and polarized HT-29 cells, by microarray analysis (Table 1) and real-time RT-PCR (Table 2). Act also caused phosphorylation of another AP-1 subunit, c-Jun, based on proteomics analysis (Fig. 4C, 4D, and 5A), and of the AP-1 activator JNK, based on Western blot analysis (Fig. 3B), in polarized HT-29 cells. Considered together, the data implied that Act activated AP-1 transcription factor activity in human intestinal epithelial cells. As shown in Fig. 6B, we confirmed Act-induced activation of AP-1 by gel shift assay, which was evident by 30 min. The observed bands were specific for AP-1, as demonstrated by competition assays.

Act induces calcium mobilization in human intestinal epithelial cells. We investigated intracellular levels of calcium in Act-treated intestinal epithelial cells. The experiments were performed in calcium-free medium in order to specifically examine release of calcium from intracellular stores. Act-treated intestinal epithelial cells exhibited a biphasic release of calcium from intracellular stores, as measured by fluorescence spectroscopy (Fig. 7). These results were similar to what we previously observed for Act-treated murine macrophages (54). The first peak of calcium release was apparent within 10 s after addition of Act to the cells and continued for 70 s before declining. The second peak of calcium release occurred at 100 s after addition of Act, which continued to increase until termination of the experiment.

Calcium is required for maximal production of IL-8 in Act-treated human intestinal epithelial cells. In order to determine whether Act-induced production of IL-8 by intestinal epithelial cells was dependent upon intracellular calcium levels, we pretreated HT-29 cells with the calcium chelator BAPTA-AM, followed by 12 ng of Act/ml, and performed ELISAs on the supernatants. As shown in Fig. 8, Act induced production of IL-8 by 8 h, as expected, which was strongly inhibited in the presence of BAPTA. Interestingly, BAPTA alone induced IL-8 production, though to a much lesser degree than Act. Compared to toxin treatment alone, addition of

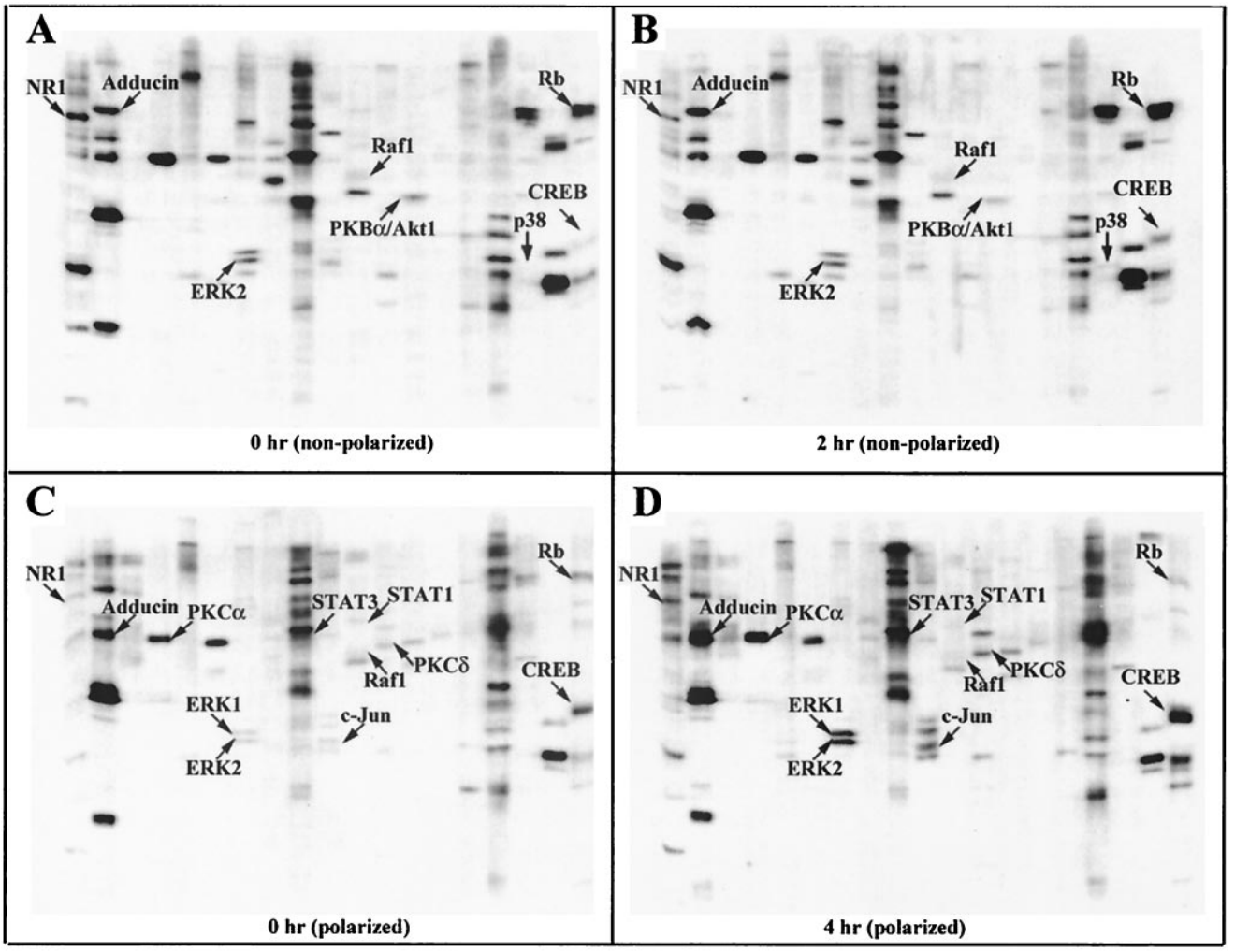

FIG. 4. KinetWorks KPSS 1.3 phosphoprotein immunoblots of whole-cell lysates from Act-treated human intestinal epithelial (nonpolarized and apical side-treated polarized) cells (HT-29). Nonpolarized cells were stimulated with 12 ng of Act/ml for 2 h, cells were lysed, and KPPS 1.3 KinetWorks protein screens were performed. Protein screens were also performed with lysates from polarized cells treated on the apical side with 50 ng of Act/ml for 4 h. Immunoblots from untreated nonpolarized control cells (A), nonpolarized cells treated with Act for 2 h (B), untreated polarized cells (C), and polarized cells apical side-treated with Act for 4 h (D) are shown. Bands corresponding to Act-induced upregulated or downregulated phosphoproteins are labeled and indicated by arrows for comparison.

BAPTA plus Act inhibited production of IL-8 by 67%. Accounting for apparent BAPTA-induced IL-8 production, there was 75% less production of IL-8 in the absence of calcium.

DISCUSSION

In this study, we demonstrated that Act altered the expression of 45 probe sets representing 34 genes in HT-29 cells (Table 1). In our previous microarray study of Act-treated RAW 264.7 macrophages (13), by using similar statistical analysis methods, we demonstrated that Act altered the expression of 76 genes. The reason for this disparity in numbers of altered genes between these two cell types is unclear. However, it is possible that Act altered the levels of a greater number of transcripts in macrophages, compared to HT-29 cells, because Act is inflammatory in nature and macrophages are professional immune cells, especially equipped to respond to bacterial products. Alternatively, initial signaling events, such as binding to a host cell receptor, may differ between these two types of cells, which requires further investigation.

Based on microarray analysis results, Act induced two genes that are known to be involved in apoptosis: Mcl-1 and TDAG51 (Table 1). Upregulation of these genes was verified by real-time RT-PCR (Table 2). There are two isoforms of Mcl-1, which belongs to the Bcl-2 family of apoptotic proteins. The longer gene product (isoform 1) inhibits apoptosis, whereas the shorter gene product (isoform 2) induces apoptosis (25). TDAG51 is a stress-associated protein that is required for T-cell receptor-dependent induction of Fas/Apo1/CD95 expression in murine T-cell hybridomas (49) and has also been shown to cause apoptosis via inhibition of protein synthesis (23). Act-associated upregulation of these genes suggested that Act induces apoptosis of human intestinal epithelial cells. We did, in fact, test that hypothesis recently and demonstrated that Act caused apoptosis of HT-29 cells and another human intestinal epithe-

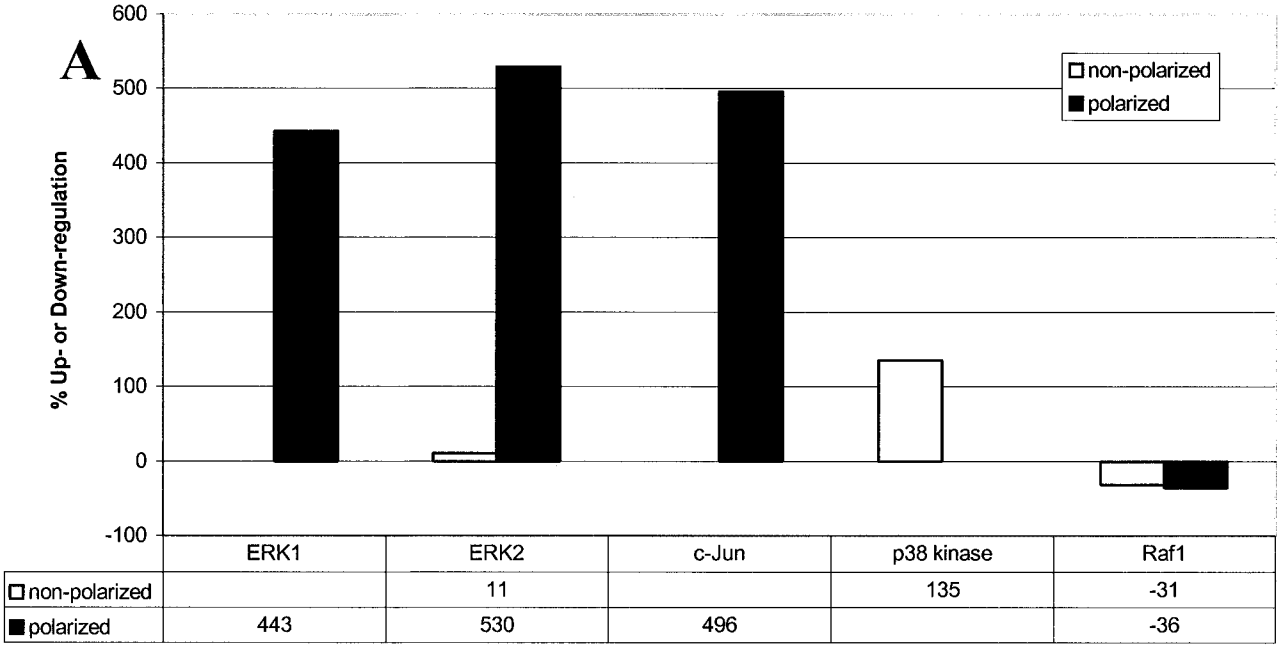

	ERK1	ERK2	c-Jun	p38 kinase	Raf1
non-polarized		11		135	-31
polarized	443	530	496		-36

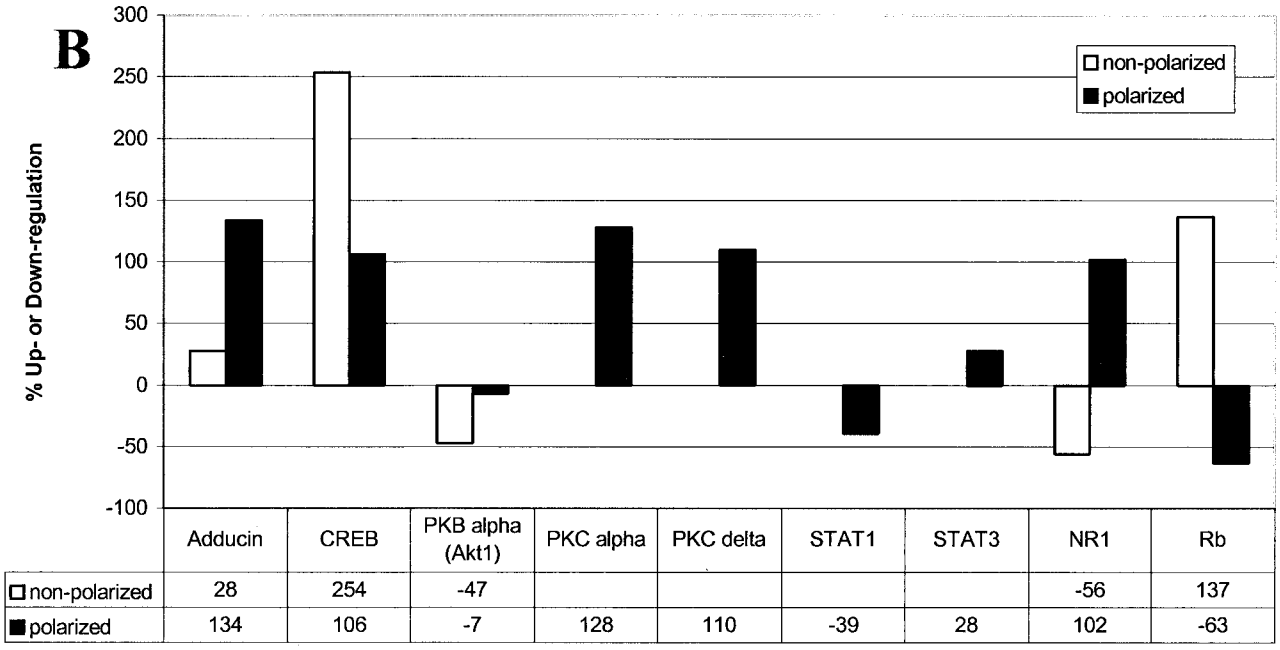

	Adducin	CREB	PKB alpha (Akt1)	PKC alpha	PKC delta	STAT1	STAT3	NR1	Rb
non-polarized	28	254	-47					-56	137
polarized	134	106	-7	128	110	-39	28	102	-63

FIG. 5. KinetWorks KPSS 1.3 phosphoprotein analysis immunoblots of whole-cell lysates from Act-treated human intestinal epithelial (nonpolarized and apical side-treated polarized) cells (HT-29). (A and B) Graphical representation of Act-induced alteration of the phosphoproteins shown in Fig. 4. Percent increase or decrease (calculated from normalized cpm values, arbitrarily based on enhanced chemiluminescence florescence intensity values) is shown in table format beneath the graph. White bars represent data from nonpolarized cells treated with 12 ng of Act/ml for 2 h; black bars represent data from polarized cells treated on the apical side with 50 ng of Act/ml for 4 h.

lial cell line (T84) (12). Coupled with cell cycle regulation (Tables 1 and 2), Act-induced apoptosis of intestinal epithelial cells carries important and obvious implications concerning *Aeromonas*-associated gastroenteritis.

Further, based on the microarray data, it seems likely that Act mediates some intestinal damage by directly altering the transcriptional profiles of the intestinal epithelial cells themselves. For example, Act induced upregulation of MMP1 at 2 and 12 h, which we verified by real-time RT-PCR (Table 2). Sustained production of MMP1 could conceivably contribute to disruption of intestinal

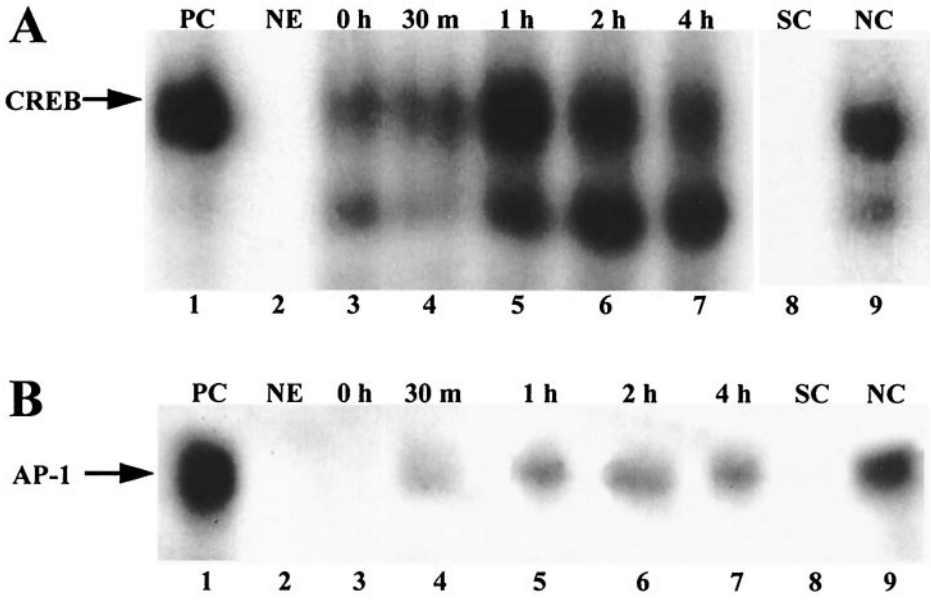

FIG. 6. Demonstration by gel shift analysis of CREB and AP-1 activation in human intestinal epithelial cells (HT-29). Act activated CREB (A) and AP-1 (B) transcription factors in polarized human intestinal epithelial cells, as determined by gel shift assay. Nuclear extracts from polarized HT-29 cells treated on the apical side with Act (50 ng/ml; 0 and 30 min and 1, 2, and 4 h) were mixed with radiolabeled consensus oligonucleotides for CREB or AP-1 and subjected to nondenaturing 4% polyacrylamide gel electrophoresis (lanes 3 to 7). Nuclear extract from HT-29 cells treated for 4 h with Act was mixed with ~50-fold excess unlabeled CREB or AP-1 consensus oligonucleotide (specific competition, lane 8) or NF-κB (nonspecific competition, lane 9) before the addition of the labeled oligonucleotide. HeLa cells extract was used as a positive control (PC, lane 1), and no extract was added as a negative control (NE, lane 2). The gel was dried and subjected to autoradiography.

tissue integrity and allow dissemination of bacteria into the lamina propria. According to the microarray analysis results, Act also upregulated urokinase-type plasminogen receptor (Table 1), which plays a role in the activation of plasminogen by binding urokinase plasminogen activator, leading to stimulation of various metalloproteases, lysis of fibrin clots, and degradation of the extracellular matrix that could result in bacterial dissemination (55).

Act also induced upregulation of genes involved in cellular

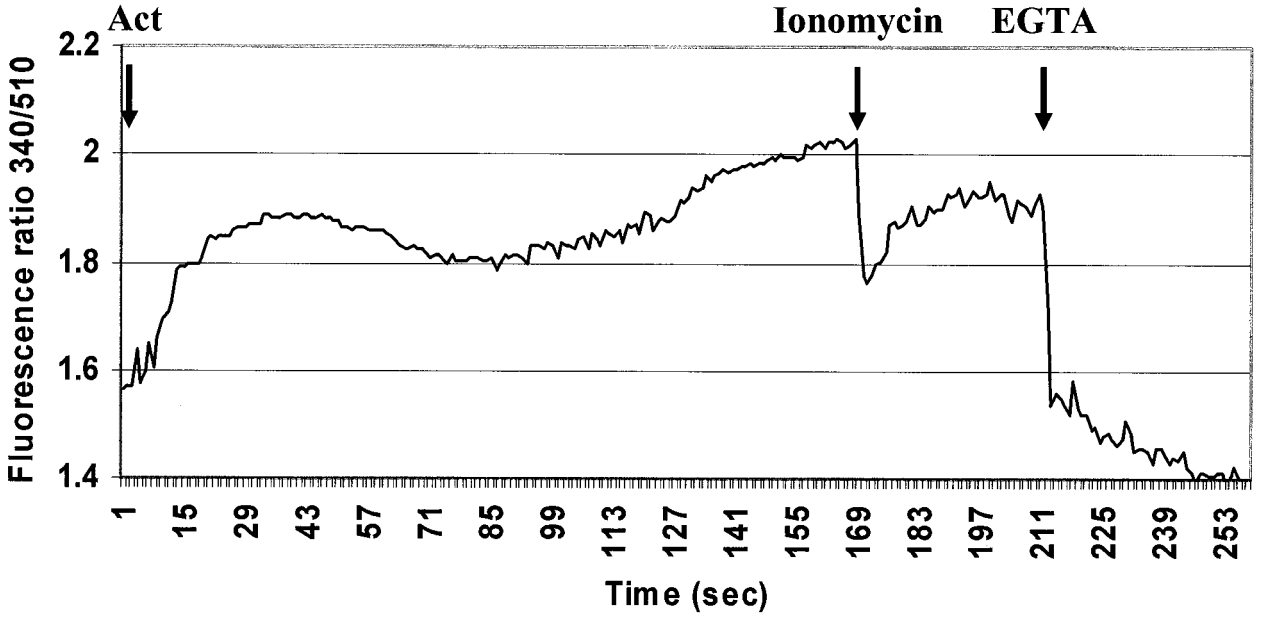

FIG. 7. Act induced release of intracellular stored calcium in human intestinal epithelial cells (HT-29). HT-29 cells labeled with FURA 2-AM were treated with 2.3 μg of Act/ml, and calcium release was measured by fluorescence spectroscopy. Biphasic calcium release from intracellular stores was noted in calcium-free medium. Three independent experiments were performed, and results from a typical experiment are shown. At the end of the experiment 1 μM ionomycin and 67 μM EGTA were added, for measuring, respectively, maximum and minimum calcium release from cells. Arrows indicate the times at which Act, ionomycin, or EGTA were added to the cells.

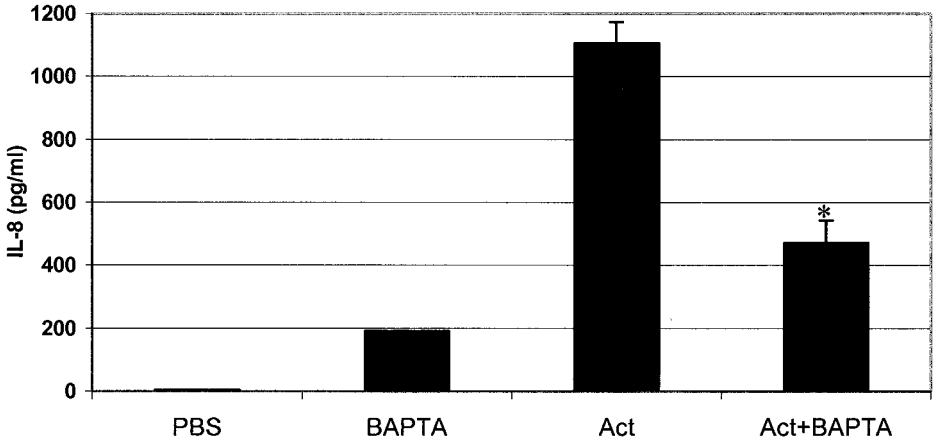

FIG. 8. Maximal production of IL-8 in Act-treated human intestinal epithelial cells (HT-29) requires calcium. HT-29 cells were stimulated with PBS or Act (12 ng/ml) for 8 h. BAPTA-treated cells (10 μM) were pretreated for 2 h before the addition of toxin. Supernatants were collected, ELISA for IL-8 was performed, and results are shown graphically. PBS alone or heated toxin (56°C/20 min) did not stimulate production of IL-8, whereas Act alone did induce production of IL-8 (1,106 pg/ml) by 8 h. BAPTA alone also induced low levels of IL-8 (192 pg/ml). As denoted by asterisk, pretreatment of cells with BAPTA significantly reduced Act-induced production of IL-8 compared to Act-treated cells alone.

reorganization (e.g., actin), migration, and cell-cell communication (Table 1) (15, 18). There were several signaling molecules and transcription factors that were upregulated in response to Act by 2 h (Table 1), including the AP-1 transcription factor subunit Fra-1, that could be involved in inflammatory responses, a situation similar to that observed in our previous study of Act-stimulated murine macrophages (13). Based on hierarchical clustering analysis (Fig. 1), Fra-1 coclustered with genes associated with cellular reorganization (i.e., connexin 31, cytokeratin 17, RhoE, and jagged 1) and cell growth (i.e., p21/Cip1, dickkopf homolog 1, and jagged 1). The similar expression pattern of these genes, as determined by clustering, suggested their involvement in the same signaling pathway or in separate but coregulated pathways. The data further implied that Act-induced cellular reorganization might involve dysregulation of the cell cycle, possibly in response to toxin-induced tissue damage.

There were four cytokine genes that were upregulated by Act, based on microarray analysis results (Table 1), which we also verified by real-time RT-PCR (Table 2) or ELISA (Fig. 2). Since Act-induced production of IL-8 by polarized epithelial cells, as determined by ELISA, only occurred when the cells were treated on the apical side, it is likely that Act initiates host signaling in human intestinal epithelial cells mainly from the apical side.

GRO1 and IL-8 are both chemotactic for neutrophils (21, 50), which suggests that Act-mediated intestinal inflammation might involve infiltration of neutrophils in addition to monocytes. Although Act did not induce upregulation of GRO1 in polarized intestinal epithelial cells, IL-8 expression was induced (Tables 1 and 2) and would likely result in the same outcome (i.e., infiltration of neutrophils into the intestinal lumen during infection). These results strongly suggested that neutrophil recruitment, via IL-8 and possibly GRO1, might contribute to *Aeromonas*-associated inflammation of the intestinal tract. How monocytes are attracted to the sight of infection is not clear but might result from the chemoattractant nature of Act (29). The combination of neutrophil and macrophage activation would likely produce a strong inflammatory response and further damage the intestinal epithelial layer. Future studies will include neutrophil responses to Act in order to determine the contribution of these cells to *Aeromonas*-associated gastroenteritis and inflammation.

In a previous study, we showed Act-induced activation of all three major MAPKs (ERK 1/2, p38, and JNK) in macrophages and in nonpolarized T84 epithelial cells (12). In the present study, we demonstrated for the first time activation of these kinases in polarized epithelial cells by Western blot analysis (Fig. 3). In order to determine what other phosphoproteins, if any, were activated by Act, we performed phosphoprotein screens of both nonpolarized and apical side-treated polarized epithelial cells. Consistent with the results obtained by Western blot analysis (Fig. 3), Act induced phosphorylation of ERK 1, ERK 2, c-Jun, and p38 in these cells within 2 to 4 h (Fig. 4 and 5). This is also consistent with our previous study of MAPK activation in Act-treated T84 cells (12). However, it is unclear why phosphoprotein screens of lysates from Act-treated polarized HT-29 cells did not reveal phosphorylation of p38, which was clearly demonstrated by Western blot analysis (Fig. 3C).

Considered together, the data indicated that Act induced phosphorylation of MAPKs in human intestinal epithelial cells, which was mediated from the apical side of polarized cells. Furthermore, we demonstrated by gel shift assay that Act activated the downstream MAPK transcription factor AP-1 in polarized epithelial cells (Fig. 6), which supported the microarray data (i.e., upregulation of the AP-1 subunit Fra-1) (Tables 1 and 2) and Western blot and phosphoprotein analyses (i.e., phosphorylation of JNK and c-Jun) (Fig. 3 to 5). Since Act was previously demonstrated to activate ERK, p38, and JNK pathways and AP-1 in murine macrophages (12), toxin-induced activation of MAPK signaling cascades might be a general mechanism of action of Act, irrespective of the cell type.

Surprisingly, Raf-1 phosphorylation was down regulated in both nonpolarized and apical side-treated polarized cells in response to Act (Fig. 4A to D and 5A). Phosphorylation/

activation of Raf-1, which is mediated by Ras, leads to phosphorylation/activation of MAPK kinase 1/2 (MEK 1/2), which subsequently phosphorylates ERK 1/2 (14, 20). Previously, in initial experiments of Act-treated RAW 264.7 murine macrophages, we noted that pretreatment with Raf antisense oligonucleotides did not ablate MEK 1 or ERK 1/2 phosphorylation (unpublished observation). Many other groups have also demonstrated Raf-independent activation of MEKs and ERKs. For instance, Schmidt et al. (58) determined that activation of MEK and ERK in primary human erythroid progenitors was mediated via Raf-independent activation of phospoinositol-3-kinase and protein kinase C (PKC). Likewise, Lad and Neet (34) demonstrated that neurotrophin receptor-induced MEK activation in fibroblasts occurred in the absence of Raf activation. Based on our results, it is likely that Act-induced activation of ERK 1/2 in murine macrophages and human intestinal epithelial cells is also mediated by a Raf-independent mechanism. How Act-induced activation of ERK 1/2 might bypass the classical Ras-Raf-MEK cascade requires further investigation.

Act caused upregulation of phosphorylated adducin in HT-29 cells. Since adducin is a critical cytoskeleton assembly factor, phosphorylation of adducin might be responsible for Act-induced cytoskeletal disorganization, which was observed in murine macrophages (12, 13). In addition, adducin-mediated alterations in sodium ion transport in intestinal epithelia exposed to Act might contribute to fluid secretion (64) and will be investigated further.

Act also upregulated phosphorylation of the transcription factor CREB in these intestinal epithelial cells (Fig. 4A to D and 5B). We verified activation of CREB in polarized cells by gel shift assay (Fig. 6). CREB, which is activated via phosphorylation by PKB/Akt, PKC, p90RSK, or p38 kinase (2, 19, 33), mediates cyclic AMP and calcium-dependent gene expression and functions in cell growth, homeostasis, and survival (39). Phosphorylation of CREB has also been associated with cellular responses to genotoxic stress (62). Act-induced activation of CREB in murine macrophages was previously demonstrated in our laboratory (5), but this is the first report of CREB phosphorylation in human intestinal epithelial cells in response to Act. Act-induced activation of CREB and also of AP-1 in human intestinal epithelial cells would contribute to host cell signaling responses to the toxin, and future studies will be aimed at determining the specific roles of these transcription factors in Act-mediated inflammation, intestinal damage, and gastroenteritis.

Other researchers have demonstrated CREB- and/or AP-1-mediated transcriptional activation of Ephrin A2 (EphA2), CCAAT/enhancer-binding protein-β, p21/Cip1, IL-8, LIF, MMP1, Mcl-1, aldehyde dehydrogenase 1, family member A3, and urokinase-type plasminogen activator receptor (6, 7, 24, 26, 27, 35, 36, 46, 47, 66–68, 74), all of which were upregulated in HT-29 cells in response to Act, based on microarray analysis results (Table 1). It is therefore likely that CREB and AP-1 are important mediators of Act-induced host cell signaling in human intestinal epithelial cells.

Act caused downregulation of phosphorylated PKBα in toxin-treated HT-29 cells (Fig. 4A, 4B, and 5B). Activation of PKBα, which occurs through phosphoinositol-3-kinase (63), results in the inactivation of apoptotic machinery components (1). Therefore, Act-induced inhibition of PKBα activity might contribute to toxin-mediated cell death. As shown in Fig. 4C, 4D, and 5B, Act increased phosphorylation of PKCα and PKCδ in apical-treated polarized intestinal epithelial cells. PKC family members phosphorylate a wide variety of protein targets and are known to be involved in diverse cellular signaling pathways (8). PKCα was shown to function as a proapoptotic factor (31, 48, 51). Likewise, PKCδ has been shown to be involved in DNA damage-induced apoptosis (43). It is unclear why Act did not induce phosphorylation of PKCα or δ in nonpolarized HT-29 cells (Fig. 4A, 4B, and 5B), but the large induction of these PKC isozymes in apical side-treated polarized cells suggests their involvement in toxin-mediated intracellular signaling and apoptosis. In addition, Act-induced activation of PKC might contribute to diarrhea via active secretion of Cl^-, which was recently demonstrated for polarized HT-29 cells treated on the apical side with beta-hemolysin of *A. hydrophila* (9).

Act treatment caused a decrease in STAT1 phosphorylation and an increase in STAT3 phosphorylation in polarized HT-29 cells (Fig. 5B). STAT1 negatively regulates the transcription of several genes, including MMP1 and c-Myc (53), whereas STAT3 activates transcription of these genes (52). The Act-induced decrease in phosphorylated STAT1 and increase in STAT3 phosphorylation (Fig. 4A to D and 5B) correlated with the observed upregulation, based on microarray analyses results, of MMP-1 and c-Myc (Table 1). Modulation of STAT signaling by Act could have profound consequences on intestinal epithelial cell responses during *Aeromonas*-associated gastroenteritis and nonintestinal infections, as it relates to tissue damage and cell death, and thus will be further explored in future.

Act treatment produced conflicting results for two proteins (NR1 and Rb) in nonpolarized and apical side-treated polarized cells (Fig. 4A to D and 5B). NR1 was down regulated (−56%) in nonpolarized cells but upregulated (102%) in polarized HT-29 cells. NR1 is a glutamate-gated ion channel with high calcium permeability and voltage-dependent sensitivity to magnesium (44, 71). Interestingly, NR1 phosphorylation was recently reported in human monocytes treated with live *Mycobacterium bovis* (22), suggesting that NR1 activity might be involved in host responses to bacterial infections. Changes in the phosphorylation status of NR1 in response to Act could contribute to alterations in intracellular Ca^{2+} levels in intestinal epithelial cells, which our laboratory is currently investigating.

Act caused upregulation of phosphorylated Rb in nonpolarized cells (137%) and downregulation in apical side-treated polarized cells (−63%). The Rb tumor suppressor protein is a potent inhibitor of cell proliferation, and phosphorylation of Rb results in Rb inactivation, which subsequently allows progression of the cell cycle. Decreased phosphorylation of Rb in Act-treated polarized HT-29 cells (Fig. 4C and D and 5B) is consistent with toxin-induced upregulation in the expression of the negative cell cycle regulator p21/Cip1 (Table 1). However, it is unclear why an increase in Rb phosphorylation was observed in Act-treated nonpolarized intestinal epithelial cells (Fig. 4A, 4B, and 5B). It is likely that the differences observed between Act-treated nonpolarized and polarized cells were due to the different time points used (2 and 4 h, respectively).

However, the opposing effects of Act on polarized and nonpolarized intestinal epithelial cells underscore the importance of cautiously interpreting data obtained by using transformed cultured cells and verifying the results in vivo.

We previously demonstrated Act-induced calcium mobilization in murine macrophages, which was derived from intracellular stores, as well as via influx from the extracellular medium (54). In addition, Act-induced calcium mobilization was implied by our immunoblotting results in the present study (Fig. 4A to D and 5A and B). For instance, Act induced phosphorylation of adducin and PKC, both of which could be mediated by calcium (32, 38, 69). Act also activated CREB (Fig. 6), which is known to mediate calcium-dependent gene expression (39), as mentioned earlier. Most compelling, Act induced changes in the phosphorylation status of the NMDA receptor, NR1, which has been shown to regulate intracellular levels of calcium in neuronal cells (3, 16, 17, 65) As expected, Act did induce calcium mobilization in human intestinal epithelial cells (Fig. 7), which could be important in the production of inflammatory mediators, such as IL-8, and crucial in the pathogenesis of *Aeromonas* gastrointestinal infections. In support of this hypothesis, we demonstrated that calcium was required for maximal production of IL-8 by intestinal epithelial cells in response to Act (Fig. 8). However, since at least 25% of IL-8 produced by Act-treated human intestinal epithelial cells occurred in the absence of calcium (Fig. 8), there probably exists an additional, calcium-independent mechanism for IL-8 production. Alternatively, calcium might serve to increase or amplify IL-8 production via a pathway that does not absolutely require calcium for minimal production.

In most cell types, regulation of IL-8 expression is typically mediated at the level of transcription (45, 46). Proximal to the IL-8 gene are three elements, recognized by AP-1, CCAAT/enhancer-binding protein (C/EBP/NF–IL-6), and NF-κB, which are known to be involved in transcriptional upregulation of IL-8 (46, 73). Because Act activated AP-1 in polarized HT-29 cells (Fig. 6B), it is likely that transcriptional upregulation of IL-8 was mediated, at least in part, by AP-1. Act-induced CREB activation might have also contributed to IL-8 production, since CREB was previously demonstrated to enhance IL-8 production in the human monocyte-like cell line U937 (26). Future studies will be aimed at definitively determining which transcription factor(s) is responsible for Act-induced upregulation of IL-8 and how calcium contributes to increased production of IL-8. Regardless of the underlying molecular mechanisms involved, Act-induced production of IL-8 by intestinal epithelial cells would undoubtedly contribute to influx of neutrophils, which would significantly contribute to *Aeromonas*-associated inflammation and gastroenteritis.

The present study provided for the first time Act-induced host transcriptional changes in nonpolarized and polarized human intestinal epithelial cells by microarray analyses. Further, proteomics approaches were used to delineate posttranslational changes in Act-treated intestinal epithelial cells. We also demonstrated calcium-dependent IL-8 production in response to Act, which was mediated from the apical side of polarized intestinal epithelial cells. Combined use of genomics and proteomics strategies allowed us to dissect signaling pathways in Act-treated host cells that could lead to tissue damage and gastroenteritis.

ACKNOWLEDGMENTS

This study was supported by a grant from the NIH/NIAID (AI41611) and the Gastrointestinal Research Interdisciplinary Program (GRIP), University of Texas Medical Branch (UTMB), Galveston, TX. C.L.G., a predoctoral fellow, obtained funding from the National Science Foundation. A.A.F. was supported by the McLaughlin Postdoctoral Fellowship, and L. Pillai, a predoctoral fellow, obtained funding from the NIH T32 Training Grant in Emerging and Tropical Infectious Diseases.

T. Wood from the Department of HBC&G at UTMB, provided the facility of his core laboratory for microarray studies. V. Reyes, from the Department of Pediatrics at UTMB, provided the facility of his core laboratory for the cytokine profile assays.

REFERENCES

1. **Ahmad, S., N. Singh, and R. I. Glazer.** 1999. Role of AKT1 in 17β-estradiol- and insulin-like growth factor I (IGF-I)-dependent proliferation and prevention of apoptosis in MCF-7 breast carcinoma cells. Biochem. Pharmacol. **58:**425–430.
2. **Cardenas, C., M. Muller, E. Jaimovich, F. Perez, D. Buchuk, A. F. G. Quest, and M. A. Carrasco.** 2004. Depolarization of skeletal muscle cells induces phosphorylation of cAMP response element binding protein (CREB) via calcium and protein kinase Cα J. Biol. Chem. M401044200.
3. **Choi, D. W.** 1987. Ionic dependence of glutamate neurotoxicity. J. Neurosci. **7:**369–379.
4. **Chopra, A. K., and C. W. Houston.** 1999. Enterotoxins in *Aeromonas*-associated gastroenteritis. Microbes Infect. **1:**1129–1137.
5. **Chopra, A. K., X. Xu, D. Ribardo, M. Gonzalez, K. Kuhl, J. W. Peterson, and C. W. Houston.** 2000. The cytotoxic enterotoxin of *Aeromonas hydrophila* induces proinflammatory cytokine production and activates arachidonic acid metabolism in macrophages. Infect. Immun. **68:**2808–2818.
6. **Chowdhury, I. H., A. Farhadi, X. F. Wang, M. L. Robb, D. L. Birx, and J. H. Kim.** 2003. Human T-cell leukemia virus type 1 Tax activates cyclin-dependent kinase inhibitor $p21^{Waf1/Cip1}$ expression through a p53-independent mechanism: inhibition of cdk2. Int. J. Cancer **107:**603–611.
7. **Conkright, M. D., E. Guzman, L. Flechner, A. I. Su, J. B. Hogenesch, and M. Montminy.** 2003. Genome-wide analysis of CREB target genes reveals a core promoter requirement for cAMP responsiveness. Mol. Cell **11:**1101–1108.
8. **Dempsey, E. C., A. C. Newton, D. Mochly-Rosen, A. P. Fields, M. E. Reyland, P. A. Insel, and R. O. Messing.** 2000. Protein kinase C isozymes and the regulation of diverse cell responses. Am. J. Physiol. Lung Cell Mol. Physiol. **279:**L429–L438.
9. **Epple, H. J., J. Mankertz, R. Ignatius, O. Liesenfeld, M. Fromm, M. Zeitz, T. Chakraborty, and J. D. Schulzke.** 2004. *Aeromonas hydrophila* beta-hemolysin induces active chloride secretion in colon epithelial cells (HT-29/B6). Infect. Immun. **72:**4848–4858.
10. **Ferguson, M. R., X. J. Xu, C. W. Houston, J. W. Peterson, D. H. Coppenhaver, V. L. Popov, and A. K. Chopra.** 1997. Hyperproduction, purification, and mechanism of action of the cytotoxic enterotoxin produced by *Aeromonas hydrophila*. Infect. Immun. **65:**4299–4308.
11. **Galindo, C. L., A. A. Fadl, J. Sha, and A. K. Chopra.** 2004. Microarray analysis of *Aeromonas hydrophila* cytotoxic enterotoxin-treated murine primary macrophages. Infect. Immun. **72:**5439–5445.
12. **Galindo, C. L., A. A. Fadl, J. Sha, C. Gutierrez, Jr., V. L. Popov, I. Boldogh, B. B. Aggarwal, and A. K. Chopra.** 2004. *Aeromonas hydrophila* cytotoxic enterotoxin activates mitogen-activated protein kinases and induces apoptosis in murine macrophages and human intestinal epithelial cells. J. Biol. Chem. **279:**37597–37612.
13. **Galindo, C. L., J. Sha, D. A. Ribardo, A. A. Fadl, L. Pillai, and A. K. Chopra.** 2003. Identification of *Aeromonas hydrophila* cytotoxic enterotoxin-induced genes in macrophages using microarrays. J. Biol. Chem. **278:**40198–40212.
14. **Geyer, M., and A. Wittinghofer.** 1997. GEFs, GAPs, GDIs and effectors: taking a closer (3D) look at the regulation of Ras-related GTP-binding proteins. Curr. Opin. Struct. Biol. **7:**786–792.
15. **Goodenough, D. A., J. A. Goliger, and D. L. Paul.** 1996. Connexins, connexons, and intercellular communication. Annu. Rev. Biochem. **65:**475–502.
16. **Grant, E. R., B. J. Bacskai, D. E. Pleasure, D. B. Pritchett, M. J. Gallagher, S. J. Kendrick, L. J. Kricka, and D. R. Lynch.** 1997. *N*-Methyl-D-aspartate receptors expressed in a non-neuronal cell line mediate subunit-specific increases in free intracellular calcium. J. Biol. Chem. **272:**647–656.
17. **Grimwood, S., E. Gilbert, C. I. Ragan, and P. H. Hutson.** 1996. Modulation of $45Ca^{2+}$ influx into cells stably expressing recombinant human NMDA receptors by ligands acting at distinct recognition sites. J. Neurochem. **66:**2589–2595.
18. **Guasch, R. M., P. Scambler, G. E. Jones, and A. J. Ridley.** 1998. RhoE regulates actin cytoskeleton organization and cell migration. Mol. Cell. Biol. **18:**4761–4771.
19. **Gustin, J. A., R. Pincheira, L. D. Mayo, O. N. Ozes, K. M. Kessler, M. R. Baerwald, C. K. Korgaonkar, and D. B. Donner.** 2004. Tumor necrosis factor

activates CRE-binding protein through a p38 MAPK/MSK1 signaling pathway in endothelial cells. Am. J. Physiol. Cell Physiol. **286:**C547–555.
20. **Hallberg, B., S. I. Rayter, and J. Downward.** 1994. Interaction of Ras and Raf in intact mammalian cells upon extracellular stimulation. J. Biol. Chem. **269:**3913–3916.
21. **Hayashi, H., M. Honda, Y. Shimokawa, and M. Hirashima.** 1984. Chemotactic factors associated with leukocyte emigration in immune tissue injury: their separation, characterization, and functional specificity. Int. Rev. Cytol. **89:**179–250.
22. **Hestvik, A. L. K., Z. Hmama, and Y. Av-Gay.** 2003. Kinome analysis of host response to mycobacterial infection: a novel technique in proteomics. Infect. Immun. **71:**5514–5522.
23. **Hinz, T., S. Flindt, A. Marx, O. Janssen, and D. Kabelitz.** 2001. Inhibition of protein synthesis by the T cell receptor-inducible human TDAG51 gene product. Cell. Signaling **13:**345–352.
24. **Iavarone, C., A. Catania, M. J. Marinissen, R. Visconti, M. Acunzo, C. Tarantino, M. S. Carlomagno, C. B. Bruni, J. S. Gutkind, and M. Chiariello.** 2003. The platelet-derived growth factor controls c-myc expression through a JNK- and AP-1-dependent signaling pathway. J. Biol. Chem. **278:**50024–50030.
25. **Iglesias-Serret, D., M. Pique, J. Gil, G. Pons, and J. M. Lopez.** 2003. Transcriptional and translational control of Mcl-1 during apoptosis. Arch. Biochem. Biophys. **417:**141–152.
26. **Ikewaki, N., and H. Inoko.** 2002. A very late activating antigen-alpha4 (CD49d) monoclonal antibody, BU49 induces phosphorylation of a cAMP response element-binding protein (CREB), resulting in induction of homotypic cell aggregation, and enhancement of interleukin-8 (IL-8) production. Microbiol. Immunol. **46:**685–695.
27. **Ikezoe, T., Y. Yang, T. Saito, H. P. Koeffler, and H. Taguchi.** 2004. Proteasome inhibitor PS-341 down-regulates prostate-specific antigen (PSA) and induces growth arrest and apoptosis of androgen-dependent human prostate cancer LNCaP cells. Cancer Sci. **95:**271–275.
28. **Janda, J. M., and S. L. Abbott.** 1998. Evolving concepts regarding the genus *Aeromonas*: an expanding panorama of species, disease presentations, and unanswered questions. Clin. Infect. Dis. **27:**332–344.
29. **Jin, G. F., A. K. Chopra, and C. W. Houston.** 1992. Stimulation of neutrophil leukocyte chemotaxis by a cloned cytolytic enterotoxin of *Aeromonas hydrophila*. FEMS Microbiol. Lett. **77:**285–289.
30. **Joza, N., S. A. Susin, E. Daugas, W. L. Stanford, S. K. Cho, C. Y. Li, T. Sasaki, A. J. Elia, H. Y. Cheng, L. Ravagnan, K. F. Ferri, N. Zamzami, A. Wakeham, R. Hakem, H. Yoshida, Y. Y. Kong, T. W. Mak, J. C. Zuniga-Pflucker, G. Kroemer, and J. M. Penninger.** 2001. Essential role of the mitochondrial apoptosis-inducing factor in programmed cell death. Nature **410:**549–554.
31. **Knox, K. A., G. D. Johnson, and J. Gordon.** 1993. A study of protein kinase C isozyme distribution in relation to Bcl-2 expression during apoptosis of epithelial cells in vivo. Exp. Cell Res. **207:**68–73.
32. **Kuhlman, P. A., C. A. Hughes, V. Bennett, and V. M. Fowler.** 1996. A new function for adducin: calcium/calmodulin-regulated capping of the barbed ends of actin filaments. J. Biol. Chem. **271:**7986–7991.
33. **Kwon, E. M., M. A. Raines, J. Blenis, and K. M. Sakamoto.** 2000. Granulocyte-macrophage colony-stimulating factor stimulation results in phosphorylation of cAMP response element-binding protein through activation of pp90RSK. Blood **95:**2552–2558.
34. **Lad, S. P., and K. E. Neet.** 2003. Activation of the mitogen-activated protein kinase pathway through p75NTR: a common mechanism for the neurotrophin family. J. Neurosci. Res. **73:**614–626.
35. **Lai, W.-C., M. Zhou, U. Shankavaram, G. Peng, and L. M. Wahl.** 2003. Differential regulation of lipopolysaccharide-induced monocyte matrix metalloproteinase (MMP)-1 and MMP-9 by p38 and extracellular signal-regulated kinase 1/2 mitogen-activated protein kinases. J. Immunol. **170:**6244–6249.
36. **Lin, W. C., B. J. Shen, Y. G. Tsay, H. C. Yen, S. C. Lee, and C. J. Chang.** 2002. Transcriptional activation of C/EBPβ gene by c-Jun and ATF2. DNA Cell Biol. **21:**551–560.
37. **Livak, K. J., and T. D. Schmittgen.** 2001. Analysis of relative gene expression data using real-time quantitative PCR and the 2(-Delta Delta C(T)) method. Methods **25:**402–408.
38. **Magnino, P. E., B. A. de la Houssaye, and R. A. Masaracchia.** 1983. Resolution and characterization of calcium/phospholipid-dependent protein kinase and H4 protease-activated protein kinase activities in lymphoid cells. Biochem. Biophys. Res. Commun. **116:**675–681.
39. **Mayr, B., and M. Montminy.** 2001. Transcriptional regulation by the phosphorylation-dependent factor CREB. Nat. Rev. Mol. Cell. Biol. **2:**599–609.
40. **McLaren, D. J.** 1970. Time, life, and boundaries. J. Paleontol. **44:**801–815.
41. **Merino, S., A. Aguilar, M. M. Nogueras, M. Regue, S. Swift, and J. M. Tomas.** 1999. Cloning, sequencing, and role in virulence of two phospholipases (A1 and C) from mesophilic *Aeromonas* sp. serogroup O:34. Infect. Immun. **67:**4008–4013.
42. **Merino, S., X. Rubires, S. Knochel, and J. M. Tomas.** 1995. Emerging pathogens: *Aeromonas* spp. Int. J. Food Microbiol. **28:**157–168.
43. **Mizuno, K., K. Noda, T. Araki, T. Imaoka, Y. Kobayashi, Y. Akita, M. Shimonaka, S. Kishi, and S. Ohno.** 1997. The proteolytic cleavage of protein kinase C isotypes, which generates kinase and regulatory fragments, correlates with Fas-mediated and 12-*O*-tetradecanoyl-phorbol-13-acetate-induced apoptosis. Eur. J. Biochem. **250:**7–18.
44. **Moriyoshi, K., M. Masu, T. Ishii, R. Shigemoto, N. Mizuno, and S. Nakanishi.** 1991. Molecular cloning and characterization of the rat NMDA receptor. Nature **354:**31–37.
45. **Mukaida, N., Y. Mahe, and K. Matsushima.** 1990. Cooperative interaction of nuclear factor-κB- and *cis*-regulatory enhancer binding protein-like factor binding elements in activating the interleukin-8 gene by pro-inflammatory cytokines. J. Biol. Chem. **265:**21128–21133.
46. **Mukaida, N., S. Okamoto, Y. Ishikawa, and K. Matsushima.** 1994. Molecular mechanism of interleukin-8 gene expression. J. Leukoc. Biol. **56:**554–558.
47. **Mynard, V., O. Latchoumanin, L. Guignat, J. Devin-Leclerc, X. Bertagna, B. Barre, J. Fagart, O. Coqueret, and M. Grazia Catelli.** 2004. Synergistic signaling by CRH and Leukemia Inhibitory Factor bridged by phosphorylated CREB at the NurRE-STAT element of the proopiomelanocortin promoter. Mol. Endocrinol. **18:**2997–3010.
48. **Nowak, G.** 2002. Protein kinase C-alpha and ERK1/2 mediate mitochondrial dysfunction, decreases in active Na^+ transport, and cisplatin-induced apoptosis in renal cells. J. Biol. Chem. **277:**43377–43388.
49. **Park, C. G., S. Y. Lee, G. Kandala, and Y. Choi.** 1996. A novel gene product that couples TCR signaling to Fas(CD95) expression in activation-induced cell death. Immunity **4:**583–591.
50. **Persson-Dajotoy, T., P. Andersson, A. Bjartell, J. Calafat, and A. Egesten.** 2003. Expression and production of the CXC chemokine growth-related oncogene-alpha by human eosinophils. J. Immunol. **170:**5309–5316.
51. **Powell, C. T., N. J. Brittis, D. Stec, H. Hug, W. D. Heston, and W. R. Fair.** 1996. Persistent membrane translocation of protein kinase C alpha during 12-*O*-tetradecanoylphorbol-13-acetate-induced apoptosis of LNCaP human prostate cancer cells. Cell Growth Differ. **7:**419–428.
52. **Qing, Y., and G. R. Stark.** 2004. Alternative activation of STAT1 and STAT3 in response to interferon-gamma. J. Biol. Chem. **279:**41679–41685.
53. **Ramana, C. V., M. Chatterjee-Kishore, H. Nguyen, and G. R. Stark.** 2000. Complex roles of Stat1 in regulating gene expression. Oncogene **19:**2619–2627.
54. **Ribardo, D. A., K. R. Kuhl, I. Boldogh, J. W. Peterson, C. W. Houston, and A. K. Chopra.** 2002. Early cell signaling by the cytotoxic enterotoxin of *Aeromonas hydrophila* in macrophages. Microb. Pathog. **32:**149–163.
55. **Romer, J., C. Pyke, L. R. Lund, J. Eriksen, P. Kristensen, E. Ronne, G. Hoyer-Hansen, K. Dano, and N. Brunner.** 1994. Expression of uPA and its receptor by both neoplastic and stromal cells during xenograft invasion. Int. J. Cancer **57:**553–560.
56. **Rose, J. M., C. W. Houston, and A. Kurosky.** 1989. Bioactivity and immunological characterization of a cholera toxin-cross-reactive cytolytic enterotoxin from *Aeromonas hydrophila*. Infect. Immun. **57:**1170–1176.
57. **Sanghera, J. S., S. L. Weinstein, M. Aluwalia, J. Girn, and S. L. Pelech.** 1996. Activation of multiple proline-directed kinases by bacterial lipopolysaccharide in murine macrophages. J. Immunol. **156:**4457–4465.
58. **Schmidt, E. K., S. Fichelson, and S. M. Feller.** 2004. PI3 kinase is important for Ras, MEK and Erk activation of Epo-stimulated human erythroid progenitors. BMC Biol. **2:**7–18.
59. **Schmitz, H., M. Fromm, C. Bentzel, P. Scholz, K. Detjen, J. Mankertz, H. Bode, H. Epple, E. Riecken, and J. Schulzke.** 1999. Tumor necrosis factor-alpha (TNFα) regulates the epithelial barrier in the human intestinal cell line HT-29/B6. J. Cell Sci. **112:**137–146.
60. **Sha, J., E. V. Kozlova, and A. K. Chopra.** 2002. Role of various enterotoxins in Aeromonas hydrophila-induced gastroenteritis: generation of enterotoxin gene-deficient mutants and evaluation of their enterotoxic activity. Infect. Immun. **70:**1924–1935.
61. **Sha, J., E. V. Kozlova, A. A. Fadl, J. P. Olano, C. W. Houston, J. W. Peterson, and A. K. Chopra.** 2004. Molecular characterization of a glucose-inhibited division gene, *gidA*, that regulates cytotoxic enterotoxin of *Aeromonas hydrophila*. Infect. Immun. **72:**1084–1095.
62. **Shi, Y., S. L. Venkataraman, G. E. Dodson, A. M. Mabb, S. LeBlanc, and R. S. Tibbetts.** 2004. Direct regulation of CREB transcriptional activity by ATM in response to genotoxic stress. Proc. Natl. Acad. Sci. USA **101:**5898–5903.
63. **Souttou, B., S. Ahmad, A. T. Riegel, and A. Wellstein.** 1997. Signal transduction pathways involved in the mitogenic activity of pleiotrophin: implication of mitogen-activated protein kinase and phosphoinositide 3-kinase pathways. J. Biol. Chem. **272:**19588–19593.
64. **Tripodi, G., F. Valtorta, L. Torielli, E. Chieregatti, S. Salardi, L. Trusolino, A. Menegon, P. Ferrari, P.-C. Marchisio, and G. Bianchi.** 1996. Hypertension-associated point mutations in the adducin alpha and beta subunits affect actin cytoskeleton and ion transport. J. Clin. Investig. **97:**2815–2822.
65. **Tymianski, M., M. P. Charlton, P. L. Carlen, and C. H. Tator.** 1993. Source specificity of early calcium neurotoxicity in cultured embryonic spinal neurons. J. Neurosci. **13:**2085–2104.
66. **Vasiliou, V., S. F. Reuter, S. Williams, A. Puga, and D. W. Nebert.** 1999. Mouse cytosolic class 3 aldehyde dehydrogenase (Aldh3a1): gene structure

and regulation of constitutive and dioxin-inducible expression. Pharmacogenetics **9:**569–580.
67. **Vincenti, M. P., L. A. White, D. J. Schroen, U. Benbow, and C. E. Brinckerhoff.** 1996. Regulating expression of the gene for matrix metalloproteinase-1 (collagenase): mechanisms that control enzyme activity, transcription, and mRNA stability. Crit. Rev. Eukaryot. Gene Expr. **6:**391–411.
68. **Wang, J.-M., J.-R. Chao, W. Chen, M.-L. Kuo, J. J.-Y. Yen, and H.-F. Yang-Yen.** 1999. The antiapoptotic gene *mcl-1* is up-regulated by the phosphatidylinositol 3-kinase/Akt signaling pathway through a transcription factor complex containing CREB. Mol. Cell. Biol. **19:**6195–6206.
69. **Weber, A., C. R. Pennise, G. G. Babcock, and V. M. Fowler.** 1994. Tropomodulin caps the pointed ends of actin filaments. J. Cell Biol. **127:**1627–1635.
70. **Wells, C. L., E. M. A. van de Westerlo, R. P. Jechorek, H. M. Haines, and S. L. Erlandsen.** 1998. Cytochalasin-induced actin disruption of polarized enterocytes can augment internalization of bacteria. Infect. Immun. **66:**2410–2419.
71. **Wisden, W., and P. H. Seeburg.** 1993. Mammalian ionotropic glutamate receptors. Curr. Opin. Neurobiol. **3:**291–298.
72. **Wittwer, C. T., M. G. Herrmann, A. A. Moss, and R. P. Rasmussen.** 1997. Continuous fluorescence monitoring of rapid cycle DNA amplification. BioTechniques **22:**130–138.
73. **Wu, G. D., E. J. Lai, N. Huang, and X. Wen.** 1997. Oct-1 and CCAAT/enhancer-binding protein (C/EBP) bind to overlapping elements within the interleukin-8 promoter: the role of Oct-1 as a transcriptional repressor. J. Biol. Chem. **272:**2396–2403.
74. **Zhang, J. W., D. J. Klemm, C. Vinson, and M. D. Lane.** 2004. Role of CREB in transcriptional regulation of CCAAT/enhancer-binding protein beta gene during adipogenesis. J. Biol. Chem. **279:**4471–4478.

Editor: J. T. Barbieri